SINTEF

Report

Numerical modelling of (thin) oil films

Improved behaviour and life time of thin films in the OSCAR model

Author(s)
Ute Brönner
Alun Lewis, Øistein Johansen, Tor Nordam

SINTEF

KEYWORDS:
OSCAR,
oil spill response,
human exposure,
thin oil films

Report

Numerical modelling of (thin) oil films

Improved behaviour and life time of thin films in the OSCAR model

VERSION	DATE
2.0	2017-09-21

AUTHOR(S)
Ute Brönner
Alun Lewis, Øistein Johansen, Tor Nordam

CLIENT(S)	CLIENT'S REF.
Petromaks 2 Thin Oil Films Steering Committee and Research Council of Norway	Cecilie F. Nygaard

PROJECT NO.	NUMBER OF PAGES/APPENDICES:
302002226	49

ABSTRACT

The PETROMAKS project *"Formation and behaviour of thin oil films and evaluation of response methods including HSE"*, in the following short "Thin oil films" has the objective to achieve new knowledge more efficient and safe oil spill response operations for releases of condensates and light crude oils that may lead to thin oil films on the sea surface. Main objectives are:

1. Increased understanding of the formation and behaviour of thin oil films .
2. Assessment of the potential human exposure to volatile compounds
3. Refined processes in oil trajectory models in order to give more reliable predictions of the life time and behaviour of thin oil films and to assess the efficacy of response options.

This report addresses objective 3. and summarizes the results of three pre-studies on important processes for modelling of (thin) surface oil. We discuss model improvements and conclude with a proposal for concrete changes in the OSCAR model to better address behaviour and lifetime of thin films in the model.

PREPARED BY	SIGNATURE
Ute Brönner	

CHECKED BY	SIGNATURE
Tor Nordam	

APPROVED BY	SIGNATURE
Mimmi Throne-Holst	

REPORT NO.	ISBN	CLASSIFICATION	CLASSIFICATION THIS PAGE
OC2017 A-181	978-82-7174-313-0	Unrestricted	Unrestricted

Document history

VERSION	DATE	VERSION DESCRIPTION
Part I	2015-07-24	Spreading of oil on the sea surface V 2.0, Alun Lewis
Part II	2015-09-30	Langmuir and Transport Modelling, FINAL DRAFT AFTER QA, Ute Brönner, Tor Nordam
Part III	2015-09-30	Solidification of waxy crude oils and condensate, Temperature adjustment of viscosity, Viscosity of waxy crude and condensates, The theory behind wax precipitation, Øistein Johansen, Ute Brönner
1.0	2015-12-11	Summary report of Part I – III
2.0	2017-08-30	Final version of report, changed to unrestricted, new report number

Table of contents

Background

The PETROMAKS project, "Formation and behaviour of thin oil films and evaluation of response methods including HSE", in the following short "Thin oil films" has the objective to achieve new knowledge for more efficient and safe oil spill response operations for releases of condensates and light crude oils that may lead to thin oil films on the sea surface. Main objectives are:

1. Increased understanding of the formation and behaviour of thin oil films and the potential for emulsion formation and solidification of condensates and light crude oils including assessment of new and improved oil spill response concepts and strategies.
2. Assessment of the potential human exposure to volatile compounds during oil spill response operations in order to characterise the risk as a function of oil composition, weathering time and sea temperature (temperate versus Artic conditions).
3. Refined processes in oil trajectory models in order to give more reliable predictions of the life time and behaviour of thin oil films and to assess the efficacy of response options.

This report addresses objective 3. and summarizes the results of three pre-studies on important processes for modelling of (thin) surface oil. We discuss model improvements and conclude with a proposal for concrete changes in the OSCAR model to better address behaviour and life time of thin films in the model. The report is structured in three parts according to the three pre-studies we conducted:

Part I: *Spreading of oil on the sea surface* describes observations of surface oil and thin oil films from field studies and real spill situations and discusses the relation of observed patterns in the slick with explanations like Langmuir circulation.

Part II: *Langmuir circulation and its relevance for oil spill modelling (with OSCAR)* takes the theory and modelling approaches for Langmuir circulation further and relates these to transport modelling with OSCAR with respect to available input data, timely and spatial resolution of the two phenomena.

Part III: *The role of rheology for surface spreading and solidification of thin oil films* looks into rheological properties of (thin) oil and processes related to these and discusses possibilities for improvement in oil spill modelling based on this knowledge.
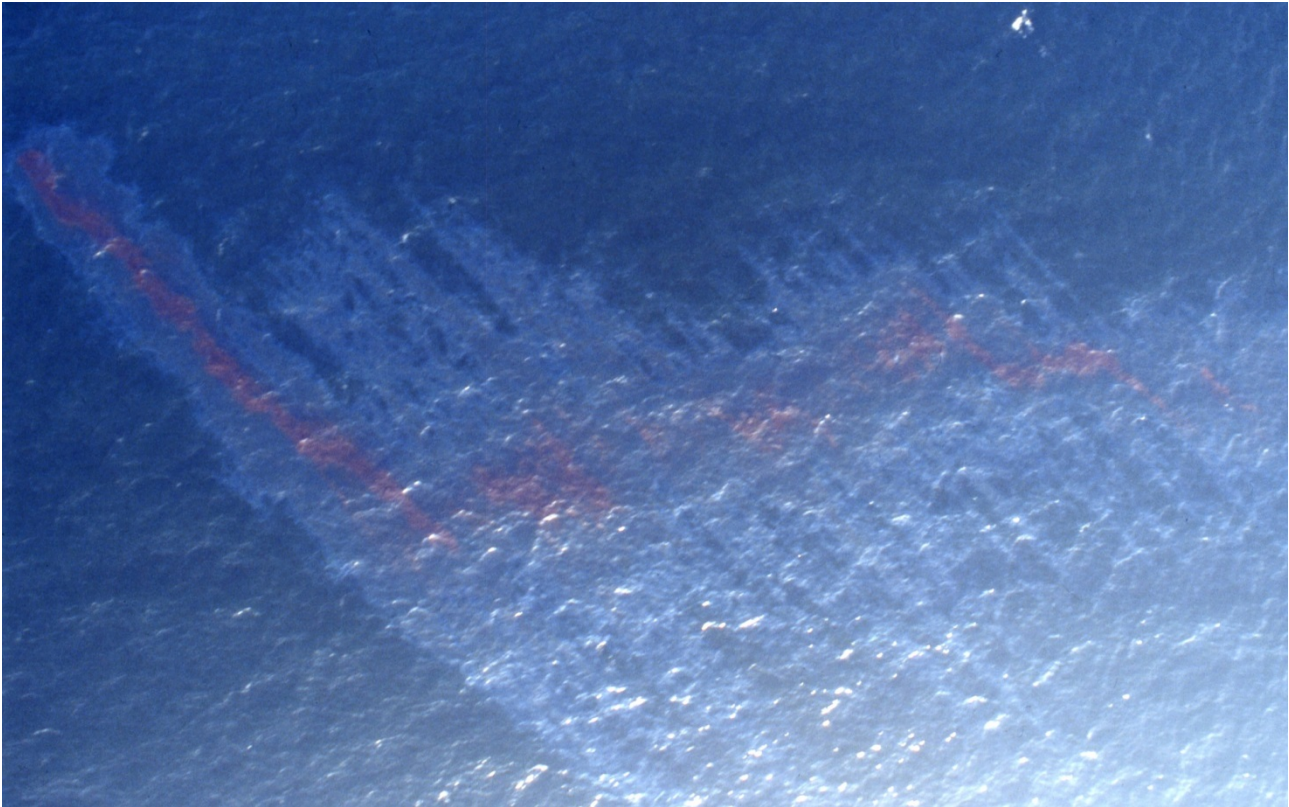
Picture courtesy: http://lms.seos-project.eu/learning_modules/marinepollution/marinepollution-c02-ws02-p01-s.html

Part I – Spreading of oil on the sea surface

The first part of the report comprises the results of a brief literature study on the appearance of surface oil during different oil spills together with a discussion on important processes for surface oil modelling, including Langmuir circulation and a first assessment of the importance of this phenomenon for transport modelling of surface oil.

1. Introduction

Crude oil on the sea surface is often observed to spread out to form slicks of very uneven thickness, ranging from barely visible sheens that are less than 1 µm (micron) thick to layers of oil that can be several millimetres or centimetres thick. The Bonn Agreement Oil Appearance Code (BAOAC), Table 1, is used to estimate oil layer thickness by visual observation.

Table 1—1 Bonn Agreement Oil Appearance Code (BAOAC)

Correlation	Description Appearance	Layer Thickness Interval (µm)	Litres per km^2
1	Sheen (silvery/grey)	0.04 to 0.30	40 – 300
2	Rainbow	0.30 to 5.0	300 – 5000
3	Metallic	5.0 to 50	5000 – 50,000
4	Discontinuous True Oil Colour	50 to 200	50,000 – 200,000
5	Continuous True Oil Colour	200 to More than 200	200,000 - More than 200,000

While visual estimation of oil layer thickness in the range of 0.04 to 50 microns can be performed with a reasonable degree of certainty, estimation of thicknesses greater than about 50 to 200 µm cannot be accurate since there are no visual effects that can be used. It should also be noted that very high viscosity oils do not spread out in the same way as low viscosity oils. The Heavy Fuel Oil released from the Erika (1999) and Prestige (2002) floated on the sea as patches that were reported to be up to 50 centimetres or more thick.

The distribution of spilled oils of low viscosity into areas of relatively 'thick' and relatively 'thin' oil thickness can be explained by the temporary natural dispersion of oil as small droplets caused by breaking waves. A breaking wave passing through the oil breaks the oil into droplets with a wide range of sizes. The buoyancy of an oil droplet is determined by the density of the oil and the size of the oil droplet and this determines the behaviour of the oil on the sea surface:

- Large oil droplets will resurface very rapidly and may float to the sea surface under the oil slick where they will coalesce with the oil slick. This process is most probably involved in water-in-oil emulsification as small water droplets can become formed and trapped in the interstices between oil droplets.

- Very small oil droplets will be retained within the water column and are considered to be naturally dispersed. These droplets will not re-join the oil slick on the sea surface, but will be subsequently biodegraded to a very large degree while in the water column.

- Oil droplets that are intermediate in size between the two sizes mentioned above will be temporarily dispersed in the upper water column. While they are submerged and subject to drift in the current, the oil on the sea surface will drift under the influence of the prevailing current **and** the wind. The temporarily dispersed oil droplets will therefore lag 'behind' the main slick. As the individual oil droplets reach the essentially 'clean' water surface they rapidly spread out to form a very thin layer of oil known as sheen or blue-shine.

Another feature that is often, but not always, observed are long, narrow linear features aligned with the wind that contain relatively thick oil separated by areas of thinner oil. The features are often referred to as 'wind rows', often contracted to 'windrows'.

Langmuir circulation is often invoked as the explanation for the formation of windrows of thicker oil, but this has not been firmly established. An alternative explanation could be that the thick / thin oil distribution is simply due to localized variations in oil thickness as the oil arrives at the sea surface that are subsequently made more apparent as the oil drifts under the influence of wind and currents, plus is subject to wave action.

2. Langmuir Circulation

The effect of Langmuir circulation (LC) on the dispersion of floating material led to its discovery by Langmuir (1938). Langmuir first studied the causes of the parallel bands, or windrows, of floating Sargassum weed he had observed during an Atlantic crossing from New York to England in 1927. The larger bands, containing 'vast' quantities of weed, with typical spacings of between 100 — 200 m, were closely aligned to the wind direction, with smaller, less distinct bands in-between. The bands realigned within 20 min of an abrupt, 90° shift in the wind direction.

LC produces the wind rows or parallel lines of foam and other floating material that appear on the surface of the sea or lakes in moderate and strong winds, and these provide evidence of the presence of the underlying circulation on the sea surface. Langmuir described the pattern of parallel vortices of alternating direction with axes aligned roughly downwind producing alternate zones of convergence and divergence at the surface, downward flows below convergence and upwards flow below divergence.
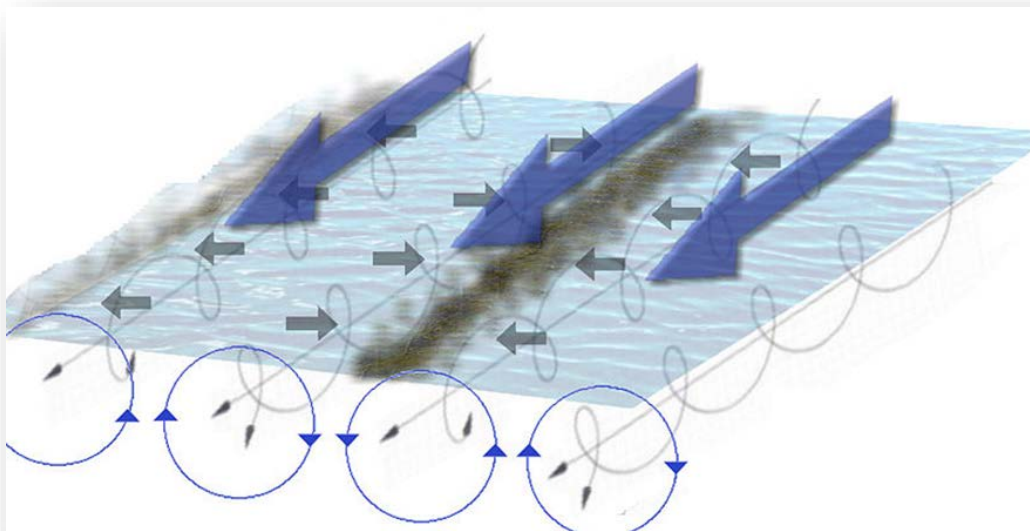
Figure 2-1 Langmuir circulation

Conditions that produce Langmuir circulation

Various forcing mechanisms have been proposed for the formation of Langmuir circulation. A full review of these is given by Leibovich (1983). The most generally accepted theory is that first suggested by Craik (1977) and further developed by Leibovich (1977) and later termed the CL2 mechanism by Faller and Caponi (1978). Theoretical and laboratory studies reviewed by Pollard (1977) and Leibovich (1983) point to a combination of waves and drift currents as being essential contributors in providing a vortex force to drive the circulation.

LC is developed when wind blows steadily over the sea surface. Smith (1992) reports that after a sudden increase in wind speed from 8 m s^{-1} to 13 m s^{-1}, prior to which there were no visible signs of Langmuir circulation, streaks with about 16 m spacing, about two thirds of the dominant wind-wavelength, were observed to form, increasing at 40 m/h for the next hour.

Spacing of windrows created by LC

Langmuir circulation may have spatial scales from a few centimetres (with capillary waves, as in Faller and Caponi 1978) to greater than 100 m (Langmuir 1938, Smith et al., 1987). Observations at sea (e.g. Smith et al., 1987; Weller and Price 1988; Smith 1992) or in lakes (Kenney 1979) show that the vortices are typically 5 - 200 m apart and lie approximately parallel to the wind direction. Langmuir circulation therefore plays a central role in 5 - 200 metre-scale cross-wind dispersion, carrying floating particles across wind into convergence regions but then impeding their further spreading until such times as the locally entrapping circulation breaks up, perhaps when one Langmuir cell merges with its neighbour, when particles may again be transferred across wind to adjacent wind rows, a mechanism first described by Csanady (1973) and later discussed by Faller and Auer (1988) and Thorpe (1992).

Faller and Auer (1988) also estimated that, when the lower boundary of the LC (i.e. water depth or depth to the thermocline) is a controlling factor, the spacing of the typical widths (*L*) of LC cells are of the order of three times the depth (*H*) of the cell.

Doppler SONAR observations from FLIP in MILDEX by Smith et al. (1987) found the ratio *L/H = 3*, the ratio staying nearly constant while *H* increased, due to the tide, from 40 to 60 m. This effect of the bottom might seem to be at variance with the observations of Faller and Woodcock (1964), but the effect can be readily explained in terms of the cascade of energy from smaller to larger scales. Many observers (e.g. Williams (1965) and Assaf et al. (1971)) have found that several scales of LCs may exist simultaneously.

Observations of Langmuir circulation in the North Sea by Graham and Hall (1997) show the ratio of windrow spacing to the water depth to be between 0.3 and 0.5. These values are typical of fetch limited, shallow seas where Langmuir circulation cells may not be fully developed, so the values for the ratio are less than those reported by Leibovich (1983) of between 0.66 and 1.66 (windrow spacing to the depth of the thermocline) in the open ocean, but similar to that given by Smith (1992) of 0.5, where the cells were still developing.

Rye (2000) briefly reviewed the factors involved and concluded that "The intention is to indicate order-of-magnitude ranges for the (spacing of) LC cells. Dependent on the factors given above, a range of order 10 - 100 metres width should be typical for oceanic conditions during reasonable winds. This range is also within that Faller and Auer (1988) indicate."

Persistence of LCs

The duration, or persistence, of individual windrows appears to vary with environmental conditions. Windrows have been found to be most persistent in the open ocean, where they have been observed to exist for periods in excess of 2 hours (Smith et al., 1987), with separations of about 100 m and down-wind lengths of 1 km. Observations from a shallow, tidally-mixed sea, show the durations to be much less: 2 — 5 min in water of 45 m depth (Thorpe et al., 1994) and about 1.5 min in water of 18 m depth (Graham and Hall, 1997). In general, the persistence of the windrows, the time between formation and destruction either by amalgamation with neighbouring windrows or break-up of the underlying circulation, was observed to increase with wind-speed.

The time-dependence and along-wind dependence of LCs both seem to be important factors for dispersion and appear to be closely related. The smaller LCs, those directly generated by wave/shear mechanism, are likely to be subject to time and space variations because of their lesser inertia. As observed by Strommel (1952), small windrows respond rapidly to gusty winds. The characteristic time scale of LC, T_C, may depend upon several factors; lateral scale, depth of penetration, undulations of the mixed layer depth and possibly hydrodynamic instabilities of well-developed LCs.

Effect of LCs on oil floating on the sea surface

Leibovich (1997) estimates that, under moderate winds and fully developed Langmuir cells, surface oil can be swept into windrows within 10 min if other forces are not effecting the slick. Based on actual spill observations, windrow formation is not evident for moderate to large spills in the first hour of the spill.

Rye (2000) examined the probable effects of LC on oil floating on the sea surface at three experimental oil spills and these are discussed in Section 5 of this report.

Many people, for example Lehr and Simecek-Beatty, 2000, consider that LCs must be involved in the re-distribution of oil floating on the sea surface. They considered that many oil spill modellers assume the wind drift factor for an oil spill is 3% of the wind speed. Observational data indicates the wind drift factor can actually vary from 1% to 6%. The higher windage may be due to oil collecting in the convergence zones of LC since surface water in this area may move at up to 5.5% of the wind speed. Unfortunately, there is not a direct relationship between wind speed and windrow velocities. This makes incorporating LC into an oil transport model difficult. Nonetheless, the authors have suggested that randomly varying the wind drift factor from 1% to 6% will better represent the distribution of observed surface oil at spills

3. Modelling of oil spreading

It is broadly recognized that the discrepancy between the modelled spreading of oil and the observations made of oil spreading at sea indicate room for improvement in the modelling. Many reviews of the modelling of oil spreading have been conducted, but a review produced by W. Lehr for CRRC at the time of the *Deepwater Horizon* incident (Lehr, 2010) identified the basic reasons for the differences between modelled oil spreading and actual oil spreading and these were considered to be:

  i.   The spreading mechanism in current models are extremely idealised, and

  ii.   The actual forces, initial conditions and boundary constraints are usually imprecisely determined.

Lehr (2010) goes on:

"Spreading of oil encompasses both the physical spreading of the oil on the top of the water and the dynamics of the surface water that is contaminated by oil. The latter can spread the surface film and also break it into pieces and allows for future coalescence. This breakage [is] a chaotic process and cannot be modelled deterministically."

Early oil spreading models used the three Fay spreading formulas, treating spreading as three phases: gravity-inertial, gravity-viscous, and surface tension-viscous. Various people have suggested modifications to the empirical coefficients used in the Fay equations, but the Fay formulas will not allow accurate prediction of slick area over any extended time period because of the neglect of outside environmental factors and details of the initial release. Even including water turbulence, Fay spreading is still incomplete. Probably the most important cause of long term oil spreading is wind stress on the slick and surface water. Unfortunately, this is a complicated phenomenon that is only partly understood.

4. Physical spreading of oil on the water surface

Oil spreads out on the sea surface to form thinner layers in a way that depends on the physical properties of the oil (principally viscosity) under the prevailing temperature and the release conditions.

The physical (and chemical) properties of the oil change at the oil 'weathers':

    i.   The oil loses the more volatile components by evaporation into the air, leaving a higher viscosity residue.

    ii.   The residue left after evaporation incorporates water droplets within the body of the oil to form a water-in-oil (w/o) emulsion with the water content increasing with time.

Under the prevailing mixing conditions provided by waves on the sea surface the water droplets are repeatedly incorporated into the w/o emulsion, but the w/o emulsion may be unstable (and likely to totally or partially) spilt into the two phases of oil and water unless asphaltenes precipitated from the body of the oil are available to stabilize the w/o emulsion. A major feature of the w/o emulsion is the much higher viscosity, compared to that of the oil from which it is formed. For many oil spill response purposes, the stability of the w/o emulsion formed by the oil is of importance. However, for the consideration of the spreading behaviour and distribution of oil on the sea surface, the emulsion stability may not be so important.

Daling et al. (2003) proposed a schematic representation where a non-emulsifying oil would continue to spread out to a thin film of sheen which was subsequently natural dispersed, whereas an emulsifying oil would increase in thickness as water is incorporated into the emulsion to form a thicker continuous slick of emulsified oil (Figure 4-1). The high viscosity of the w/o emulsion would inhibit further spreading and the emulsified slick would gradually break down into progressively smaller pieces of w/o emulsion on the sea surface. The eventual fate of the small pieces of w/o emulsion would be to be converted into tar-balls.
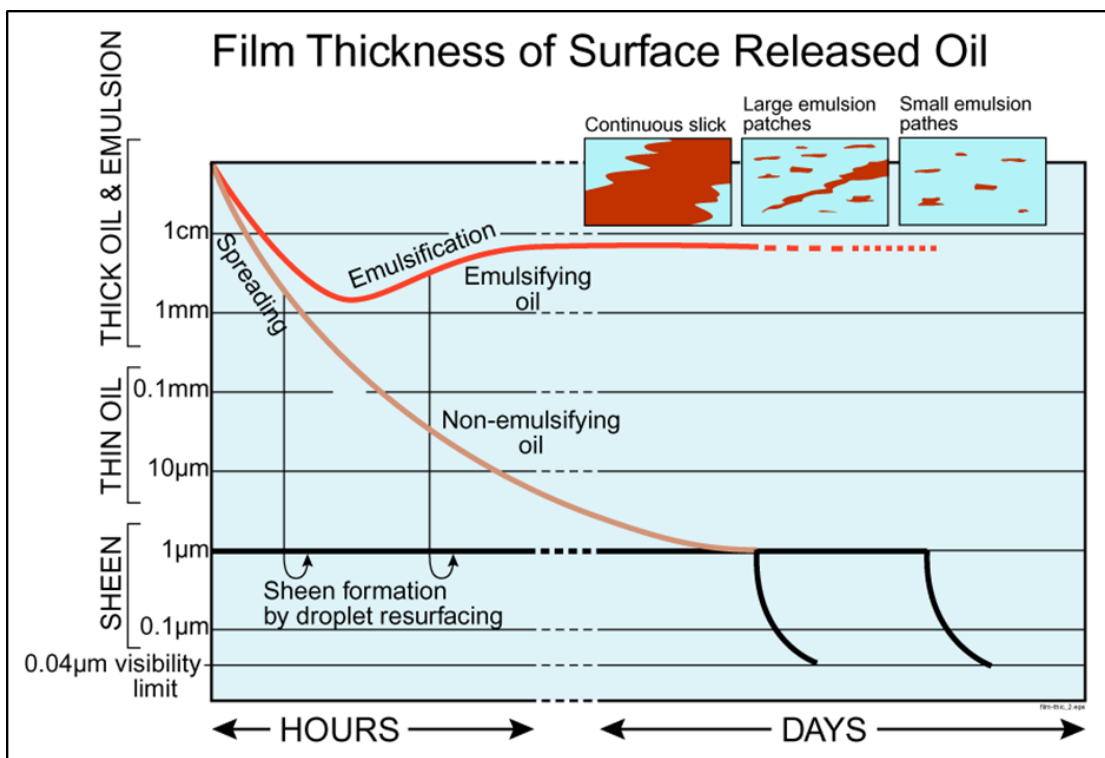

Figure 4-1 Film thickness of surface released oil (from Daling et al. (2003))

5. Case studies of observations of oil on the sea surface at real oil spills

5.1 Torrey Canyon

The *Torrey Canyon*, laden with 117,000 tonnes of Kuwait crude oil, ran aground on the Pollard Rock 15 miles west of Land's End (Cornwall, UK) on 18th March 1967. The tanker had been travelling at about 16 to 17 knots when it struck the rocks and six oil storage tanks were torn open during the grounding. Crude oil begun to escape from these tanks and within approximately 9 - 10 hours a narrow oil slick approximately 8 miles (13 km) long was drifting in the 15 to 20 knot northerly wind. It was estimated that 30,000 tonnes of oil was released into the sea in the first 2 to 3 days and 48,000 tonnes was released in the first week. The wind speed increased to gale force (33 to 40 knots) and the ship began to break up. The ship was bombed by Buccaneer aircraft of the Fleet Air Arm on 28th, 29th and 30th March. The remains of the ship sank below the sea surface towards the end of April.

Black and white photographs taken at the time show very dark coloured oil flowing into the sea from the grounded ship. The behaviour of the spilled oil at sea was not studied in immense detail. The drift of the oil was plotted to estimate where it might drift ashore. The focus of attention was on the effects the oil could cause when it came ashore.

Oil began to arrive on the Cornish coast about five days after the grounding and by this time the oil was heavily emulsified. The spilled oil at sea continued to drift under the tidal conditions at the western end of the English Channel under the changing wind directions and speed. A large portion of the oil drifted towards the coasts of northern France. The beaches of the north coast of Brittany received about 15 - 18,000 tonnes of oil which arrived on 10th -12th April over about 60 miles of coast, about 3 weeks after it had been released into the sea. On May 12th, a large patch of oil consisting of "*floating pieces of oil of varying sizes up to 'rafts' of some 100 square metres with a thickness of perhaps 10 - 15 cm and of the consistency of heavy grease*" was observed and tracked. This oil came ashore around the Pointe du Raz and the Crozon peninsula, south of Brest, on 19th and 20th May, almost 2 months after it had been released into the sea.

An interpretation of observations

The Kuwait crude oil that was spilled from the *Torrey Canyon* would have rapidly weathered to produce stable w/o emulsions on the sea surface. These may, or may not, have formed windrows at sea. Reliable observations are not easily available, although the oil slicks were monitored by aircraft while they were at sea. It is obvious that some proportion of the oil remained on the sea surface for an extended period of 8 weeks and it remained in the form of relatively large patches of emulsified oil in multi-centimetre thicknesses. The emulsified oil was not all broken up into smaller pieces with an eventual, long-term fate of being converted into tar-balls.

5.2 Ekofisk Bravo blowout

The apparent effect of unstable w/o emulsions on the spreading behaviour of oil on the sea surface was convincingly demonstrated at the *Ekofisk Bravo* blow-out on April 22nd, 1977 (Audunson, 1977).

The oil and gas was ejected from a pipe 20 metres above the sea surface on the platform and into the air. Because of the probability of ignition of the oil and gas, the oil was sprayed, as it passed through the air, with large amounts of seawater. The oil arrived on the sea surface as a mixture of oil and seawater and very rapidly formed a w/o emulsion under the prevailing sea conditions in a 20 knot wind. The w/o emulsion contained 71% volume water, but was unstable losing 20% volume water after standing still for 2 hours. Most of the oil on the sea surface was in the form of this unstable w/o emulsion.

There was no continuous, coherent oil slick, but a large collection of long, narrow emulsion strips with a thickness ranging from 1 - 20 mm. Each strip could be up to 1 - 2 km, having a width of 10 m. Inspection showed that the detailed structure of the strips of w/o emulsion was of smaller strips. The outer edges of the strips often broke down into smaller, pea-sized lumps varying from 0.5 - 1 cm to 4 - 5 cm in diameter. The

lumps had the same consistency as the strips. The lumps 'melted' together again upon mutual contact or upon contact with a larger slick. The distance between the strips in smaller areas near the platform could be under 10 m, while the distance between the strips in the central portions of the slick was most often from 100 - 1,000 m.

In large areas around the emulsion strips, a thin oil film with a thickness of 0.001 - 0.01 mm was observed. This film, characterized as 'blue shine' was difficult to observe from ships but could be observed from aircraft - best in the surface area bordering clean water

After the blowout stopped on 30th April, the wind subsided and it became relatively calm for 1 to 2 days. This resulted in large sections of the emulsion strips breaking down. The oil on the sea surface weathered in the strong sunlight and the viscosity increased. When the wind again rose from 2nd May, strips of w/o emulsion were once again formed and were significantly more stable than the w/o emulsion previously formed. The w/o emulsion was more brown in colour than that previously observed. After a relatively short time, the emulsion strips were broken down into smaller lumps from 0.2 - 2 cm in diameter. The water content of these lumps varied from 50 - 60%. Observations on 15th May of the remaining 'oil slicks' showed characteristic strips of oil lump collections with a usual size of 1 - 6 m. The concentration of lumps was estimated at approximately 30 lumps per square metre.

An aerial IR photograph taken on 28th April with a 20-knot wind showed strips of relatively thick w/o emulsion about 500m long and about 20 - 30 metres wide separated by 70 to 150 m 'clear' strips of thinner oil.

An interpretation of observations

The formations of long, narrow strips of unstable w/o emulsion aligned with the wind occurred initially occurred at relatively high wind speeds of around 20 knots. The high viscosity of this unstable w/o emulsion, combined with the relatively high wind speed, seems to have been the relevant factors leading to the formation of the strips of emulsion.

When the wind speed decreased, the unstable w/o emulsion started to lose water and this would have decreased the viscosity of the w/o emulsion. The emulsion spread out to thinner layers and the discrete strips became less prominent. The relatively high air temperature of around 24°C and fairly intense sunlight caused the viscosity of the oil residue to increase. The crude oil had already lost

5.3   Deepwater Horizon / Macondo

The subsea release of oil and gas at the *Deepwater Horizon / Macondo* incident caused the oil to reach the sea surface as relatively thin layer of oil. Due to the long duration of the oil release and the complex currents in the Gulf of Mexico, the oil on the sea surface rapidly became a mixture of freshly released oil and much 'older' weathered and emulsified oil that had a characteristic orange-red colour (Figure 5-1).

Figure 5-1 Oil on the surface of the Gulf of Mexico at the Deepwater Horizon / Macondo incident (picture courtesy SINTEF)

The distribution of oil floating on the surface varied due to the prevailing conditions which varied from nearly flat calm to hurricane force winds during the progress of the incident,

Figure 5-2 shows the windrows of emulsified oil that were formed and Figure 5-3 shows emulsified oil being concentrated at a convergence zone.

Figure 5-2 Oil on the surface of the Gulf of Mexico at the Deepwater Horizon / Macondo incident (picture courtesy SINTEF)
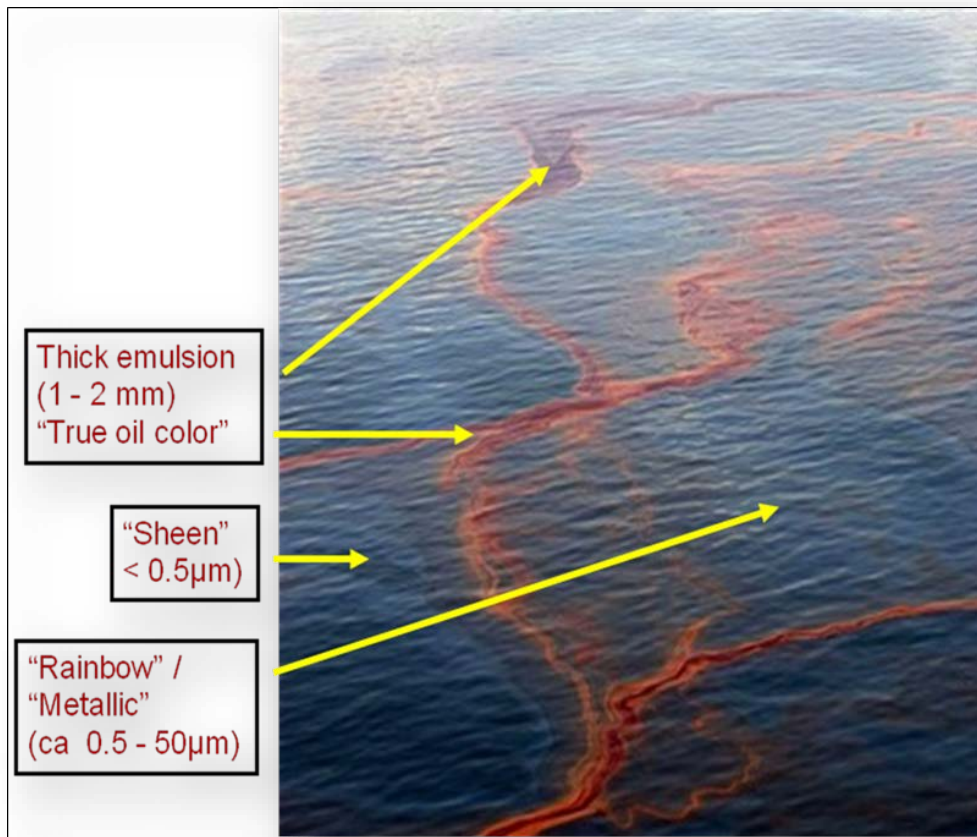

Figure 5-3 Oil on the surface of the Gulf of Mexico at the Deepwater Horizon / Macondo incident (picture courtesy SINTEF)

5.4 Heidrun platform, Haltenbanken, July 7th 2003

Oil is sometimes observed floating on the sea surface in the vicinity of offshore oil installations due to 'upsets' in the oil / water separators that control the amount of oil in the produced water that is routinely released into the sea at depth. Such an incident occurred at the Heidrun platform at Haltenbanken in July 2003. The platform had problems with the hydrocyclones and produced water with a high oil content was released into the sea. The small oil droplets at low concentration in the produced water floated up to the calm sea surface.

The Norwegian authorities operate a surveillance aircraft equipped with a variety of sensors to detect oil pollution and the oil floating on the sea surface was initially observed to consist of a very thin layer (Figure 5-4).

Figure 5-4 Oil on the sea surface at Haltenbanken on July 7th 2003 (picture courtesy SINTEF)

Over the next two days the majority of the oil was naturally dispersed from the sea surface, but the small amount of oil that remained was in the form of small strips of emulsified oil (Figure 5-5). There was clearly some mechanism that allowed the initially very thin layer of oil to be redistributed in broadly parallel strips on the sea surface and the oil layer was thick enough for the oil to become emulsified.

Figure 5-5 Oil on the sea surface at Haltenbanken on July 9th 2003 (picture courtesy SINTEF)

6. Observations of oil on the sea surface at selected experimental oil spills

Rye (2000) examined the probable effects of LC on oil floating on the sea surface at three experimental oil spills:

1) 100 tonnes of oil in 1982 (surface release at Haltenbanken 1982),
2) 30 tonnes of oil in 1989 (surface release at Haltenbanken 1989) ,
3) an underwater release of 40 m^3 of oil in the North Sea in 1996.

6.1 Haltenbanken 1982

100 tonnes of Statfjord crude oil was released onto the sea surface on 25th July 1982 (Audunson et al., 1984). The oil on the sea surface rapidly formed windrows of emulsified oil.
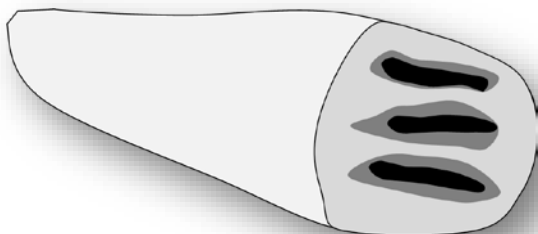

Figure 6-1 About 6-8 hours after spillage. Emulsion forms "windrows" at the front of the slick (figure SINTEF)
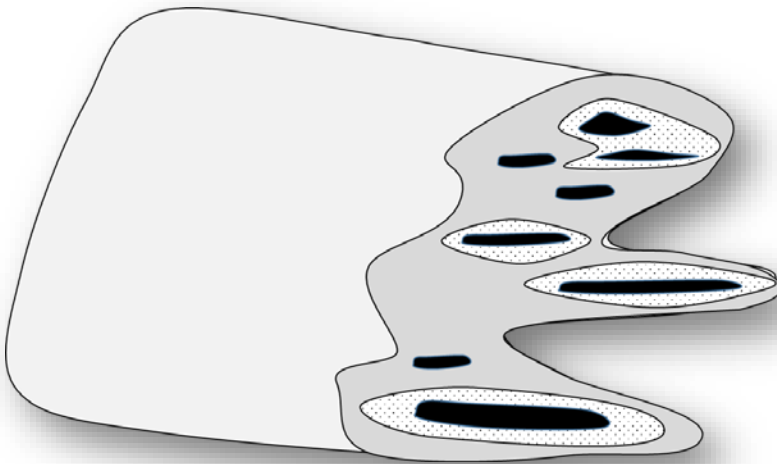
Figure 6-2 1 - 4 days after spillage. The emulsion stripes are more pronounced (figure SINTEF).

The thicker parts of the slick were measured as being 8 - 9 mm thick and consisted of emulsified oil with a water content of 80% volume. The water column was stratified at about 30 - 50 metre water depth. Rye considered that the spacing of the parallel lines of emulsified oil, at 200 to 400 metres apart was too large to be caused by LC, because the spacing predicted by Faller and Auer (1988) would have been 60 - 75 metres.

6.2   Haltenbanken 1989

30 tonnes of Oseberg crude oil was released onto the sea surface on July 1st 1989 (Sørstrøm et al., 1989). The prevailing wind speed decreased from 7 m/s to 3 - 4 m/s during the 12 hours after the oil was released onto the sea surface and the wind direction is indicated by the green arrow in the images below.

Figure 6-3 is an aerial photograph of the oil slick taken about 12 hours after the release. The thicker part of the slick (the darker coloured central portion) was about 2 km long, 100 m wide. The thickness was around 7 mm and the oil was emulsified, containing about 80% volume water. There are no apparent effects due to LC.
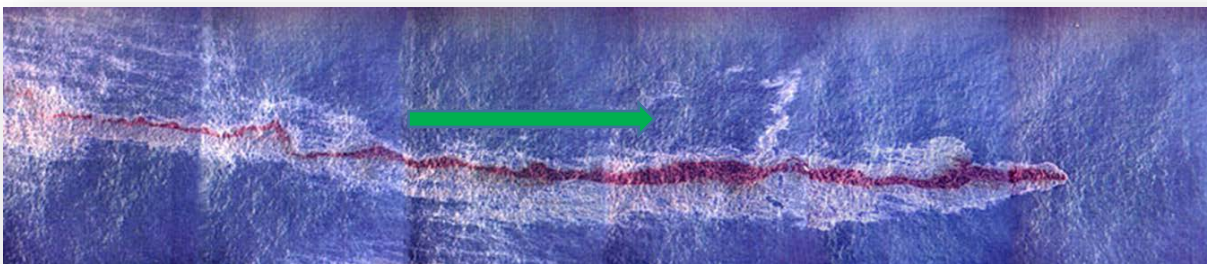
Figure 6-3 Oil on sea surface 12 hours after release (picture courtesy SINTEF).

After about 18 hours of the oil drifting at sea there was an abrupt change in wind direction from north-west to south-west (as indicated by green arrow) and the wind speed remained low at about 4 - 5 m/s. Figure 6-4 is an aerial photograph taken 24 hours after oil release. The overall slick length had increased to approximately 4 km by this time. The change in wind direction had cause the slick to break up into a series of smaller slicks, aligned almost parallel to each other.

Figure 6-4 Oil on the sea surface 24 hours after release (picture courtesy SINTEF).

Rye concluded that the spacing between the slicks, being approximately 100 metres, was again too large to be explained by LC formation. With a stratification depth of 25 metres, the spacing between LC cells predicted by Faller and Auer (1988) should have been approximately 25 metres.

6.3 Underwater release 1996

An experimental underwater release of oil and air was carried out in June 1996 close to the Frigg field in the North Sea. 40m^3 of Troll crude oil was released from the seabed at a depth of 106 metres over a period of 40 minutes. The subsurface release with air caused the oil to rise as oil droplets together with the bubbles of air. A detailed description of the release can be found in Rye et al. (1997).

When the plume of oil droplets and air bubbles reached the sea surface, the oil spread out over a large area (Figure 6-5). The wind velocity during the release was 9 to 10 m/s with the wind from the west to north-west. The significant wave height was close to 1.8 metres. The stratification (vertical profile of temperature and salinity) in the water column was measured and showed the presence of a salinity gradient at 25 - 50 metre water depth.

Figure 6-5 is an aerial photograph of the oil floating on the sea surface during the release. Using the BAOAC the oil appearance would be classified as "Metallic", indicating that the oil thickness was in the range of 5 to 50 microns. Measurements made from sampling boats indicated that the thickness was between 10 and 40 microns.

PROJECT NO.
302002226

REPORT NO.
OC2017 A-181

VERSION
2.0

19 of 49

Figure 6-5 Oil (and air) rising to the sea surface with the oil spreading out to form a thin film (picture courtesy SINTEF).

An aircraft equipped with IR (Infra-red) and UV (Ultra-Violet) sensors monitored the sea surface during and after the oil release. IR detects the thicker layers of oil and UV imaging detects all the oil without any discrimination of oil thickness.

Figure 6-6 shows the IR and UV images of the oil just after the release finished. The yellow arrow on the IR image shows current direction and the green arrow shows the wind direction. The IR image shows evidence of LC cells with the spacing being about 30 - 40 metres. Rye noted that this "[…] probably reflects the presence of LC cells. […] This cell distance appears to be within the expected range, and it also matches the criterion that the cell width is bounded by the stratification depth."
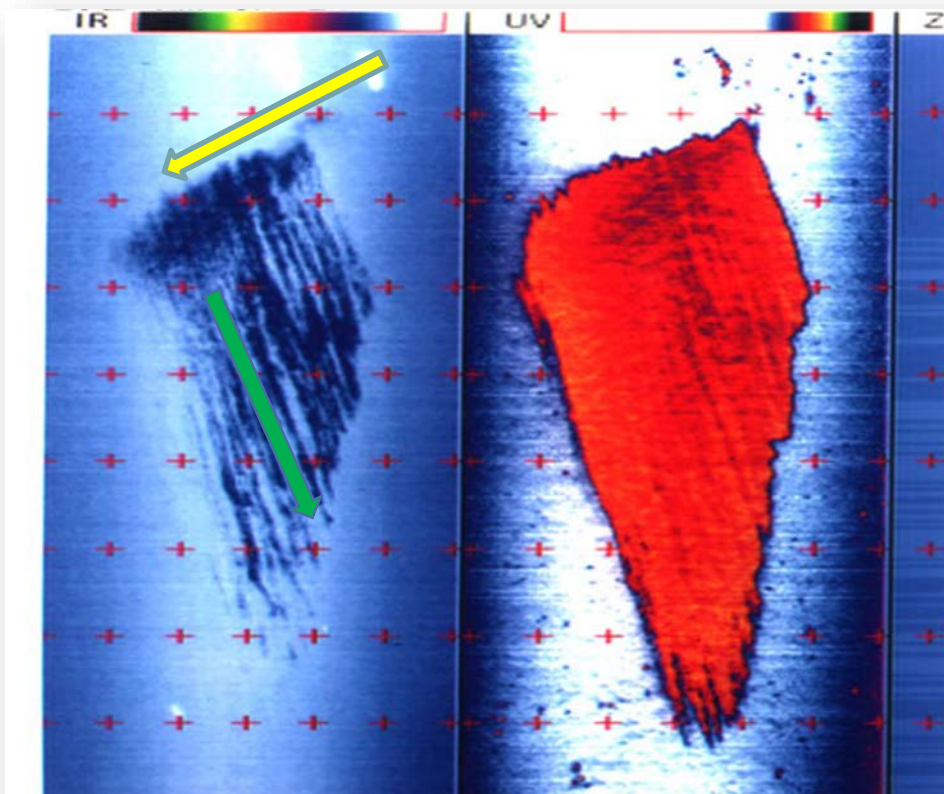
Figure 6-6 IR and UV images of oil on sea surface as release finished. The yellow arrow shows current direction and the green arrow shows the wind direction (picture courtesy SINTEF).

7. Conclusion

LC (Langmuir Circulation) Cells

Oil on the sea surface has often been observed to form long, narrow strips of oil, often called wind rows or windrows, where the oil is thicker than the surrounding oil.

One of the probable reasons for this effect is the formation of LC cells in upper water column that leads to convergent and divergent zones with floating oil being concentrated to thicker oil layers in the convergent zones and the oil layer thinned in the divergent zones. However, the formation of LC cells requires a steady wind with more than a minimum speed and should result in the spacing of the resulting parallel strips of oil being between 10 and 100 metres. In addition, LC cells are not permanent features and will only persist for a relatively limited time before breaking down, although they may reform later.

If an oil layer was initially of even thickness of a particular value, say 50 µm (micron), the oil thickness in the 'thick' oil windrows would be increased by a factor of three or four to 150 µm or 200 µm, while the oil thickness in the remainder of the oil slick wold be decreased to 10 or 20 µm, or less. This LC mechanism for the formation of windrows of thicker oil is very plausible, but is only circumstantial and has not been confirmed by measurement because measuring the actual oil layer thickness at sea is difficult.

Some observations of oil floating on the sea surface in the form of parallel strips if thicker oil with much thinner oil in between seem to conform to what would be expected from the effects of LC cells, but in other cases the strips of thicker oil are at a greater spacing than can be explained by LC cell formation. Other

processes, such as the concentration of oil near convergence zones present in other circumstances may also be responsible for the formation of narrow strips of thicker oil.

Attempts to model the behaviour of oil floating on the sea surface under the influence of Langmuir circulation (LC) would need to simulate the formation of the Langmuir cells. This appears to be challenging as not all the relevant factors seem to be known.

W/o emulsification

W/o emulsification of oil is not a prerequisite for long, narrow strips of thicker oil to be formed by Langmuir circulation; any floating material will be concentrated into windrows. The high viscosity and cohesive nature of many w/o emulsions is not relevant to initial windrow formation by Langmuir circulation. However, the windrows of oil often observed at real oil spills are most often of emulsified oil.

Whether this a consequence of the oil initially being concentrated into thicker layers by Langmuir circulation is difficult to determine. Very thin oil layers, perhaps less than 10 or 20 µm thick, will be broken up by the inclusion of water droplets by wave action into the body of the oil. There must be a minimum oil layer thickness for w/o emulsification to occur, but this varies with oil type (Melbye et al. 1999). An oil layer of 100 to 200 µm thick will easily be able to incorporate a significant volume of water droplets that are 50 µm in diameter. Once w/o emulsification has started, there will be an equilibrium of entrainment of water droplets caused by wave action and a coalescence of water droplets to sizes that are great enough to separate out of the w/o emulsion. The smaller oil droplets will be retained in the body of the oil, but the w/o emulsion will be unstable unless precipitated asphaltenes from the oil are present to stabilize the w/o emulsion.

The thickness of an emulsified layer of oil will increase in proportion to the volumetric water content; an oil layer that was initially 100 µm thick might decrease to 75 µm due to evaporative loss from the oil, but will then gradually increase to 300 µm thick as 75% volume of water is incorporated.

The following three factors could improve long-term modelling of the spreading of oil behaviour on the sea surface:

1. Langmuir circulation in the upper water column needs to be implemented in the models. This will obviously only be possible if the basic processes of Langmuir circulation can be modelled and the appropriate environmental inputs of wind speed and direction interacting with current speed and direction are available.

2. The localized effects of wind stress on the oil slick and on the surface water need to be considered. This will tear the oil film into smaller pieces or concentrate the oil into locally thicker layers. These oil layer thickness variations will then be responsible for subsequent changes. Lehr (2010) suggests that eddy diffusion coefficients are incorporated into the modelling or simulating the effect by random displacement of separate Lagrangian elements that simulate the oil (as e.g. included in OSCAR).

3. An elastic component in the flow behaviour of w/o emulsions, both the stable w/o emulsions formed by precipitation of asphaltenes from the oil, and the unstable emulsions that are formed under the prevailing wave conditions. Determining the viscoelastic flow properties of a stable w/o emulsion is challenging. Determining the viscoelastic flow properties of an unstable w/o emulsion that only exists under the wave conditions required to produce it will be even more difficult.

Picture courtesy: http://www.ldeo.columbia.edu/~ant/Langmuir.html

Part II – Langmuir circulation and its relevance for oil spill modelling
(with OSCAR)

This second part will continue the work from the first part, taking a more detailed look at the OSCAR model and the surface processes included, together with a more thorough assessment of Langmuir circulation (LC) and possibilities for implementation. There is particular attention to the effect of LC in drawing buoyant material (e.g. floating foam, algae or oil) into bands or 'windrows' on the water surface. The obvious question is if modelling of Langmuir circulation needs to be included into the modelling of oil transport, in particular if the effects of LC will affect the behaviour of thin oil films in a way that oil might accumulate to film thicknesses relevant for processes like emulsification.

8. Langmuir Circulation, previous work, theory and implementation

Langmuir (1938) was the first to observe and publish a study of the phenomena of accumulation in 'windrows', bands of floating material aligned parallel to the wind. Numerous observations have since been made of the organized counter-rotating vortices with axes aligned roughly with the wind (within 30°) and associated with a three-dimensional, cell-like circulation. These cells are now known as Langmuir cells and the circulation as Langmuir circulation (LC). Figure 8-1 and Figure 8-2 sketch some of the features of Langmuir circulation and dispersion of flotsam (from Thorpe, 2000).

8.1 Conditions for Langmuir circulation

Langmuir cells appear to be almost everywhere in the upper ocean (but not in shallow waters) and occur in nearly all, except nearly calm, conditions of wind speed. They cause diverging and converging flows at the sea surface and downward motion below the windrows, while there is upward motion in the diverging zone (Thorpe, 2000). All investigators agree that forming of windrow is a very rapid process (within minutes after a rapid shift in wind direction).
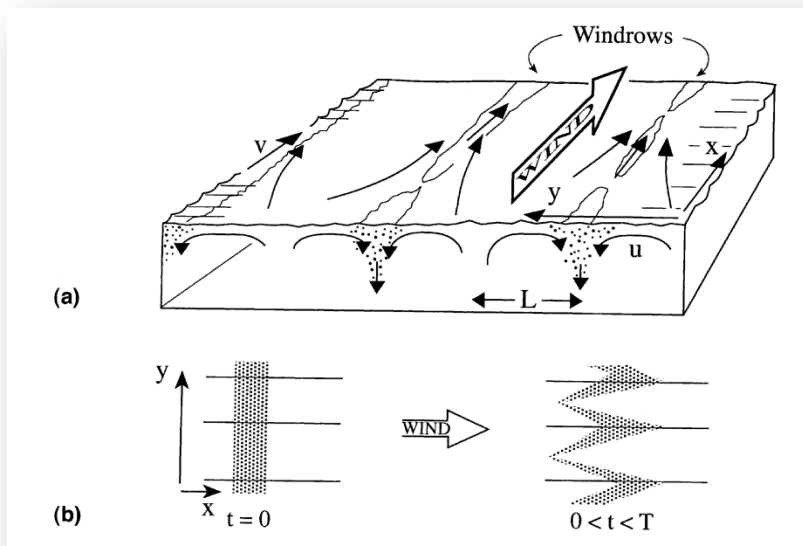
Figure 8-1 Some of the features of Langmuir circulation (from Thorpe, 2000). (a) Perspective sketch. Axes x and y are down and across wind. Slowly rising buoyant particles or small bubbles may be accumulate in the convergence regions below the floating bands of windrows; (b) longitudinal dispersion and advection of floating particles by Langmuir circulation. Distributions are sketched in plan-form at start time $t = 0$ and at a later time $t > 0$, but before cells become unstable or merge, typically at a time T.

PROJECT NO.
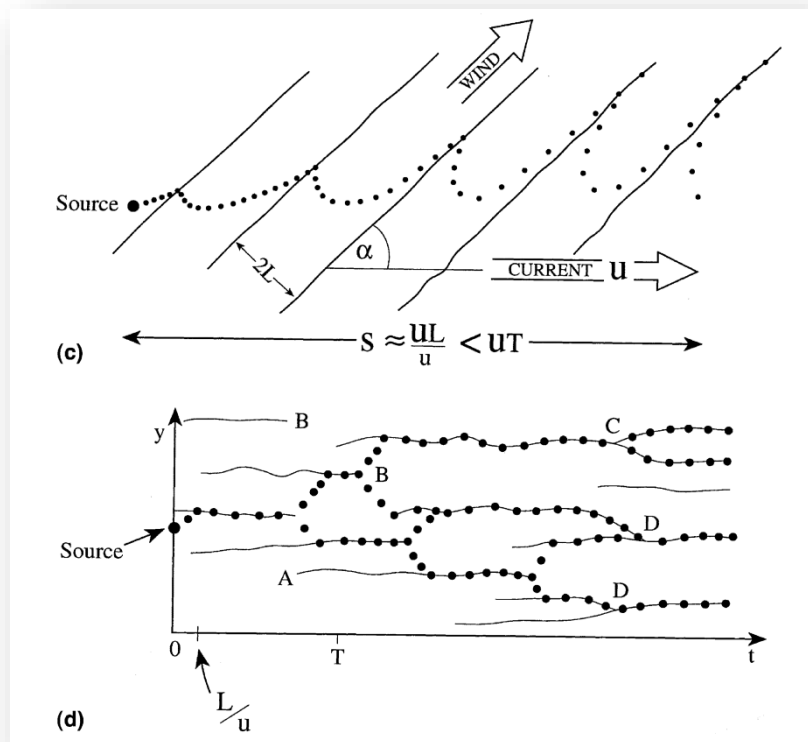302002226

REPORT NO.
OC2017 A-181

VERSION
2.0

24 of 49

Figure 8-2 Some of the features of Langmuir circulation (from Thorpe, 2000) – cont.
(c) advective dispersion of a plume of floating particles originating from a source (marked) when the wind and mean current are inclined at angle α. The planform sketch shows the windrows as lines and the particles as dots, advected by the mean current U, and by the surface velocity field of the Langmuir circulation; (d) dispersion of floating 'particles' by Langmuir circulation break-up or instability. The $y - t$ plane is sketched, advancing in x. Windrows are shown by the lines, and the tracks of 'particles' released at time $t = 0$ by dots. Windrows are formed (e.g., at A), terminate (e.g., at B) where 'particles' are left to spread to neighbouring windrows, bifurcate (e.g., at C) and amalgamate (e.g., at D). No attempt is made to represent the reduction in 'particle concentration' with y or t.

Craik and Leibovich, and their co-workers (for review see Leibovich, 1983) have produced the most generally accepted theory to explain the generation of the vortices or Langmuir cells, and there are now numerical models which describe their evolution and stability (e.g. (McWilliams & Sullivan, 2000; Nimmo-Smith, 2000; Skyllingstad, 2000).

Langmuir circulation is driven by wind as is turbulence in the ocean mixed layer (OML). As wind generates waves on the sea surface these will result in a current along the wave direction (Stokes drift) with

$$u(z) = U_s e^{2kz} \tag{8-1}$$

with U_s being its magnitude at the surface (z = 0), k the wavenumber and z the depth ($z \leq 0$).

The wind stress generates a vertical shear in the ocean mixed layer with a friction velocity

$$u_* = \sqrt{\tau_s/\rho}, \tag{8-2}$$

PROJECT NO.
302002226

REPORT NO.
OC2017 A-181

VERSION
2.0

25 of 49

τ_s being the surface stress and ρ being the sea water density. The interaction between Stokes drift and wind-driven shear produces a vortex force that generates the Langmuir circulations (Craik and Leibovich, 1976, from Yang, Chamecki, & Meneveau, 2014). The relative strength of Langmuir circulation and shear turbulence is measured by the turbulent Langmuir number

$$La_t = \sqrt{u_*/U_s}. \tag{8-3}$$

Langmuir circulation is frequently studied with so-called large-eddy-simulations (LES), a mathematical model for turbulence used in computational fluid dynamics. LES operate on the Navier–Stokes equations to reduce the range of length scales of the solution, reducing the computational cost. LES was assessed too cumbersome for frequent scientific uses and practical applications like oil spills (McWilliams & Sullivan, 2000).

8.2   Stability of Langmuir cells

The close relation with the surface wind and wave field makes Langmuir cells inherently transient events. Cells persist for even shorter durations in variable wind conditions. A second factor is cell scale which seems to be dependent on water or thermocline depth, whichever is shallower. However, the effect of depth is less clear as can be seen from the observations given in Table 8—1. An approximate relation between cell spacing L and water or thermocline depth D is given within the range $2/3 < L/D < 5/3$. A correlation between wind speed W and spacing L was reported as L = 4.8s • W (Leibovich, 1983).

A summary of selected observations is given in Table 1:

Table 8—1 Observations of duration times T, of cells of dimension L, in wind speeds W.

Location	Depth (m)	W (m/s)	L (m)	T (min)	Reference
Southern North Sea	18 B	4-15	2-6	~1.5	Graham and Hall (1997)
Southern North Sea	45 B	5-10	5-15	2-5	Thorpe et al. (1994)
Lake of Woods	3-4 B	3-9	6	~60	Kenney (1977)
Str. of Georgia	20-50 T	8-13	5-25	> 6	Farmer and Li (1995)
Northern Pacific	40-60 T	15	60-90	~120	Smith et al. (1987)
Loch Ness	10-30 T	3-22	6-10	20-30	Thorpe et al. (1994)

Durations of 2-5 min were found in 45 m water depth by Thorpe et al. (1994. Much longer times of 20-30 min were found in the deep and stratified Loch Ness with a thermocline depth of 10-30 m. Smith et al. (1987) report 1 km-long cells of 100 m separation in the ocean which persisted for periods of 2 hours, and in water of about 3 m depth in the shallow Lake of the Woods, Kenney (1977) found windrows to persist for periods of about 1 h, and to have downwind extent some 100 times L.

Nimmo-Smith (2000) found with an analytical solution under steady conditions that Langmuir circulation contributes significantly to the lateral dispersion when the wind speed is over approximately 10 times the current speed, the angle between current and wind is between 30⁰ and 120⁰ and the Langmuir cells are stable enough for the material to reach the windrows. McWilliams & Sullivan (2000) demonstrated the importance of Langmuir circulation for vertical mixing in turbulent regimes and proposed to use K-Profile Parametrization (a simplified model of vertical transport and mixing) for predicting the behaviour of spilled material in the ocean.

Lateral (cross-wind) dispersion of oil or other buoyant material transported by windrows is a function of the lifetime and strength of the Langmuir cells. Lifetime is the mean time interval between initial formation of a Langmuir cell and its break-up, *T*, and the time between local material transfer events. The process of moving

PROJECT NO.
302002226

REPORT NO.
OC2017 A-181

VERSION
2.0

26 of 49

material across wind is characterised by a cross-wind diffusion coefficient of order L^2/T. L is the spacing between windrows. Recent study of Langmuir circulation has therefore focussed less on the mechanisms of its generation and more on its instability or the disruption of cells, and the consequent dispersion to which this leads.

8.3   Effects of Langmuir circulation on sea surface oil

The most obvious dispersal effect of Langmuir circulation (LC) is to carry floating material into bands, causing a local concentration of material. On reaching the windrows the buoyant material is trapped until the local circulation breaks up or merges with adjacent cells. The time scale for transfer of material is *L/u* (with *L* being the spacing between cells and *u* the converging speed), typically about a minute. In the usual conditions in which the wind and the sea-surface (possibly tidal) mean current are not parallel, an oil plume issuing from a point source is spread across-current as a consequence of the differential advection within cells, themselves carried by the mean current past the source. This advective, cross-current dispersion is a function of the angle between the wind and the mean current.

LC produces a vertical downward transport in the windrow convergence zones and a vertical upward transport in the intervening divergent zones. Vertical dispersion in these different zones might therefore be considered equally and independent from buoyancy due to droplet sizes. Downward transport of weakly buoyant material in these convergence zones is also a possibility, and could have a significant influence on dilution and horizontal dispersion (Yang et al., 2014). However, a more important effect for oil might be the down-wind horizontal transport of oil on the sea surface. Surface drift is usually assumed proportional to the wind drift, with a rate of 3-4% of the wind speed. It is known that water masses in windrows move faster than the water between windrows. Oil gathered in windrows is affected by the underlying water motion in this region rather than the average water motion (Leibovich, 1997) and may move at up to 2% faster than the average water velocity.

The break-down or merging of the LC vortices determines their longer-term effect on horizontal dispersion, or at least on the across-wind dispersal of a patch of floating material such as oil. The array of cells is generally unsteady, with individual cells surviving for only finite times before breaking down or amalgamating with their neighbours. When this happens, material caught in a windrow is carried into, and merges with the neighbouring windrow. Farmer & Li (1995) used underwater sonar to detect the bands and describe the geometry of the so-called 'Y-junctions' where bands amalgamate.

Simecek-Beatty & Lehr (2000) have identified three areas where Langmuir circulation may be important for spill behaviour:

1. Surface spreading,
2. dispersion of droplets in the water column,
3. transport of the mass centre of the slick,

and reviewed the standard approaches to modelling these processes in common oil spill models. The following chapter describes how these processes are modelled in OSCAR before we relate these to Langmuir circulation modelling.

9.   Oil transport in OSCAR

The SINTEF Oil Spill Contingency and Response (OSCAR) model is a 3-dimensional model system that calculates and records the distribution (as mass and concentrations) of contaminants on the water surface, on shore, in the water column and in sediments. For subsurface releases (e.g. blowouts or pipeline leakages), the near field part of the simulation is computed with a multi-phase integral plume model embedded in OSCAR. Oil in OSCAR is represented by numerical particles, or pseudo-Lagrangian elements (LE). They are pseudo-Lagrangian in the sense that they are acted on by multiple processes and forces, including wind and wave action and have variable size. A surface LE may be entrained as a droplet cloud in the water column due to

natural or chemical dispersion, and will in general lose some of its mass due to evaporation of volatile and dissolution of soluble components (Johansen, Rye, & Cooper, 2003; Johansen, 2000; Reed, Brandvik, et al., 1999).

9.1 Surface spreading (advection)

The surface slick in OSCAR is simulated by a pseudo-Lagrangian model. Spreading occurs due to gravitational forces (size and area of an individual pseudo-Lagrangian particle) and horizontal turbulent dispersion (advection of the pseudo-Lagrangian particles). Entrainment and subsequent re-surfacing under the combined action of wind and waves also contribute significantly to spreading of the surface slick.

Random walk spreading of Lagrangian elements (advection)

The random walk formulation is based on Csanady (1973), employing a diffusion coefficient which increases with particle age. The random walk process results in increased separation among the LE's.

Dispersion in the water column and subsurface spreading

Oil droplets may be dispersed into the water column by natural dispersion due to breaking waves (Johansen, Reed, & Bodsberg, 2015; Delvigne et al 1988 and later) or via chemical dispersion. Dispersion contributes to surface spreading because of subsequent resurfacing of larger droplets.

The turbulent contribution of Langmuir circulation is not implemented in the current version of OSCAR. The assumption is that the breaking waves will dominate the turbulent regime for entrainment and droplet formation and long term averaged turbulence by wind and waves will dominate vertical mixing and advection.

9.2 Surface transport

The transport of a surface Lagrangian element in open water is calculated from a number of contributors:

- The surface layer of the input current data used for the modelling.
- A random contribution to simulate turbulent diffusion.
- Wind velocity proportional to a windage factor.
- Outward current contribution from a surfacing plume, if relevant.

Stokes drift is not implemented as a contributor in the current version of OSCAR, but may be so in the near future. Wave data from a wave model will then be required as input data to the oil spill model.

10. Possible ways to include Langmuir circulation in OSCAR

There are two approaches to include Langmuir circulation in an oil spill model:

1. Model Langmuir circulation cells externally and have the results as additional input and forcing data for the relevant transport processes.
2. Include possible effects of Langmuir circulation into relevant transport processes without modelling the phenomenon itself (i.e. parameterisation).

10.1 Modelling of Langmuir circulation

Langmuir circulation occurs at length scales on the order of 10 or 100 meters. These are typically much smaller than the resolution of the wave and current data used for oil spill modelling, and smaller than what one can reasonably expect to resolve in an ocean circulation model for the time being. We can therefore not expect to find Langmuir cells as part of the input data to oil spill modelling. The LES modelling methods applied else-where are too computationally intensive to include in today's oil spill models. Thus, Langmuir circulation would have to be represented in a parameterization within OSCAR, by using analytical expressions to obtain

additional terms to be added to the current field, when the wind and current conditions are such that Langmuir cells are expected to form.

Number of Lagrangian elements

If the contribution from Langmuir circulation could be added to the current field at a reasonable resolution, oil spill models (OSCAR) would in principle be able to simulate windrows as it is, as the convergence and divergence zones of the current field would tend to gather Lagrangian elements in rows. However, there are a number of practical problems:

- Lagrangian elements representing surface oil in a typical OSCAR simulation tend to be relatively large in diameter compared to the scale of Langmuir cells. For windrows at a separation of 100 m to be observed, Lagrangian elements would have to be of the same size or smaller.
- In order to produce small-sized Lagrangian elements one would have to use a very large number of particles, which is computationally prohibitive in the present version.

Moving to larger numbers of particles is part of our software roadmap, but requires some design, development and verification work to make sure everything works as expected.

Computational time step

The implementation of diffusion in OSCAR uses a hybrid representation, where Lagrangian elements increase in size with time, and a random walk component is added to the movement of each Lagrangian element. These random steps can be considerably longer than the length scale of separation of wind rows, unless extremely short computational time steps are used.

High resolution grids

In order to represent windrows explicitly in the surface grid, the gridded model area would require a resolution in the tens of meters or less. In many realistic cases this will increase computational requirements or demand significant changes in the software development of the model.

10.2   Parameterised representation of windrows

A simpler approach than a true mechanistic simulation of windrows could be to identify the conditions in which Langmuir cells are likely to form, and to estimate their size and stability based on theory and observations. From this assessment, possible effects of Langmuir circulation like converging of material into windrows, increased vertical mixing, and enhanced transport in windrows could be included into the modelled processes or not.

For example, the formation and spacing of possible windrows within one time step and grid cell can be estimated from available input data and in those cases it might be assumed that the surface oil coverage is a fraction of the coverage without windrows being present. The exact fraction depends on the estimated strength and persistence of the Langmuir cells. The adjusted coverage will result in an "effective thickness" which can be applied per Lagrangian element for processes like emulsification, evaporation, and entrainment. The definite implementation (and testing) of this has not been determined at this point of time.

10.3   Coupling of three dimensional transport and fate of oil spill simulation with wave-induced circulation

Liu & Sheng (2014) coupled wave-induced circulation and oil spill behaviour by using a circulation model called CH3D (Curvilinear-grid Hydrodynamics in 3D) combined with the wave model SWAN. The hydrodynamic model incorporated several advanced schemes of radiation stress and vortex force formulations and limited physical and chemical processes affecting the oil spill. Processes such as weathering, particle size

distribution, multiple phases including gas and hydrates were not considered in the oil spill process model employed.

An experiment was conducted in a basin with 100 m length, 100 m width and 10 m depth and the results were compared to the simulation. The horizontal grid spacing in the simulation was 1 m, with 10 vertical layers. The simulation used 0.2 s time step for a period of 10 min. Y-shaped junctions could be observed in the simulated bands, which is qualitatively consistent with the observations by Farmer and Li (1995).

While this example showed the possibility to couple wind, wave and oil spill modelling to account for effects of Langmuir circulation, the spatial and temporal resolutions exceed the usual resolutions used in oil spill and risk assessment modelling by far, as discussed above.

11. Conclusion

From the brief literature review summarised above we derive typical spatial scales for Langmuir cells of some tens to hundreds of metres. Windrows occur at time scales of a few minutes to a few hours (observations in Table 8—1 are on the order of minutes), the upper range being roughly comparable to one time step in a typical current dataset used for oil spill modelling. Length scales tend to be much smaller than the resolution of most current datasets. Representation of Langmuir effects in oil spill modelling will therefore require spatial and temporal resolutions for input data which are significantly higher than those usually available.

Given that explicit inclusion of Langmuir circulation in the OSCAR model is not feasible at present, the approach has to be indirect inclusion of the effects of the processes:

1. Surface spreading: assessing the probability for oil dispersed into windrows will allow for computing a probable coverage and thickness distribution. This procedure needs to be designed, implemented, and tested.
2. Dispersion into the water column: natural dispersion is modelled via breaking waves which will probably dominate the turbulent regime when present. Natural dispersion and turbulence in calm conditions where Langmuir circulation dominates will alter the transport of oil droplets in the water column. This transport pathway will have to be added to the model. .
3. Mass transport: Increased down-wind velocity in windrows and lower velocity in divergence zones leading to the prominent fingered representation of surface oil needs very high resolution in the oil spill model. While LES easily resolve these phenomena, they cannot be resolved in model simulation areas typically covering tens or hundreds of kilometres.

12. Recommendation

Langmuir circulation probably affects the thickness and distribution of oil on the sea surface, and is therefore a potentially important process which is not included in OSCAR or other oil spill models today. Representation of the effects of windrows relies on improved implementation of surface spreading, entrainment, subsea transport, resurfacing and transport on the sea surface. Specific issues that require improvement are:

1. Gravity spreading, which is implemented to be independent of oil viscosity and ambient temperature in the present model;
2. Spreading by entrainment, subsea transport, and resurfacing needs to be revised to align with ordered subsurface transport as created by Langmuir cells;
3. Behaviour of solidified oil on the sea surface.

Further improvement of OSCAR with respect to handling wave data as input in addition to wind and current fields will enable better assessment of the probability for Langmuir cells and wind rows and will allow including their effects in the modelled processes. Thickness and time required for emulsion formation as a function of wind speed needs to be further established. These developments are outside the scope of the present project.

We therefore recommend focusing on improving the above listed issues, and allocate the inclusion of Langmuir effects to a separate project.

Mathematical Models for Flow Behavior

Newtonian	$\sigma = h\dot{\gamma}$
Shear thinning	$\sigma = K\dot{\gamma}^{\,n}$ $(n<1)$
Shear thickening	$\sigma = K\dot{\gamma}^{\,n}$ $(n>1)$
Bingham	$\sigma = \sigma_o + \eta_p\dot{\gamma}$
Herschel-Bulkley	$\sigma = \sigma_o + K\dot{\gamma}^{\,n}$
Casson	$\sigma^{1/2} = \sigma_o^{1/2} + \eta_\infty^{1/2}\dot{\gamma}^{1/2}$

σ = shear stress; $\dot{\gamma}$ = shear rate; σ_o = yield stress; $\eta_{p,\infty}$ = limiting viscosity

from http://www.iq.usp.br/mralcant/About_Rheo.html

Part III – The role of oil rheology for surface spreading and solidification of thin oil films

Part III discusses rheological properties of (thin) oil together with related processes in the fate of oil on the sea surface and in the water column and proposes possibilities for improvement in the modelling of oil spreading based on this knowledge.

13. Modelling of spreading & transport on the sea surface

Oil on the sea surface will spread through the mechanisms of gravity and surface tension, limited by the effect of viscous retardation, and transported due to combined effects of waves, winds, and currents.

The classical spreading equations developed by Fay (1971) and Hoult (1972) describe three distinct phases for the spreading of oil in clam conditions:

1) The initial spreading rate is controlled by gravity and inertial forces.
2) Later (or for thinner slicks) the spreading rate depends on the balance between gravity and viscous (water (!) viscosity) forces.
3) At very late times (or for very thin slicks) spread is forced by surface tension and controlled by viscous forces.

(Fanneløp & Waldman, 1972). Mackay et al. further developed the gravity-viscous equation into a model of a thick layer feeding a thinner layer (Gjøsteen, 2001). The main observations which are not reflected in a Fay type of spreading are described by Reed, Johansen, et al. (1999) and include

- Formation of elongated slicks, with different film thicknesses (a thick film "feeding" a thin slick)
- Reduced spreading of viscous oils
- The break-up of oil slicks into patches after the spreading of the slick itself has terminated
- The difference in spreading according to the type of the discharge
    o Instantaneous versus continuous
    o Surface vs. subsurface

The OSCAR model represents oil on the sea surface as "spillets", a circular representation of an oil mass with information like mass (oil & emulsion), water content, position, thickness, radius and more. Gravity spreading is calculated for each spillet and a uniform thickness assuming friction between the water and the oil layer being the force which opposes spreading. Like the Fay model, OSCAR includes the viscosity of sea water but not the oil viscosity and distinguishes light and heavy oils via oil density in the model formulation. An approach to include oil viscosity has been proposed by introducing a velocity gradient (Venkatesh, El-Tahan, Comfort, & Abdelnour, 1990) to account for vertical shear resistance in relation to oil viscosity.

Several improvements to the Fay-type models have been attempted and their advantages and disadvantages are discussed in Reed et al. (1999). The main point for criticism is the neglect of environmental factors which are presumed to dominate spreading for long-term spills. Another argument is that only the second (and third) phase happen in the time frame for response (Lehr, 2001).

Proposed improvements for modelling of surface oil included

- Modifications of the Fay model for the effects of oil viscosity and the termination of spreading. This requires computation of the oil viscosity at different temperatures and weathering states and solutions for that are discussed in chapter 14.
- Linking surface spreading to natural dispersion, sub-surface spreading and resurfacing (to account for the recognized physics after the gravity-viscous phase) like implemented in OSCAR.
- Distinction between instantaneous and continuous spills with respect to the direction of the spreading and differences in slick thickness like implemented in OSCAR.

In addition, we will discuss the implications of solidified oil on the sea surface in chapter 15.

14. Viscosity of oil and oil emulsions, non-Newtonian behaviour and established measuring and modelling methods

Viscosity is the measure of a substance's resistance to motion under an applied force.

Dynamic (absolute) viscosity is the relation of the force (shear stress τ) required to move a horizontal plane with respect to another plane at a velocity (shear rate $\dot{\gamma}$) to this velocity while maintaining a distance apart in the fluid:

PROJECT NO.
302002226

REPORT NO.
OC2017 A-181

VERSION
2.0

33 of 49

$$\tau / {\dot{\gamma}} = \mu \qquad (14\text{-}1)$$

where μ is the dynamic viscosity of the fluid (Newton's law). The unit is usually given in centipoise (g / cm s or $1/10$ N s/m^2). Fluids that follow this relation are called Newtonian. For non-Newtonian fluids the relation is more complex (see Figure 14-1).
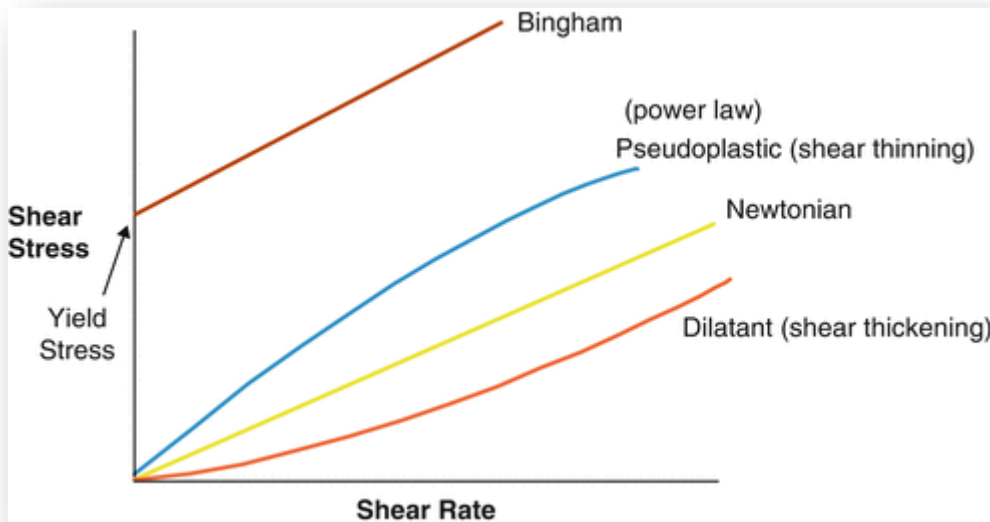

Figure 14-1 Shear stress vs. shear rate for Newtonian and Non-Newtonian Fluids

It is well known that the viscosity of waxy crudes will show non-Newtonian behaviour at temperatures below the wax appearance temperature (WAT), see paragraph 14.1 below. Viscosity is dependent of temperature in general, with viscosity (of fluids) being lower at higher temperatures and higher at lower temperatures.

The *kinematic* viscosity is the ratio of dynamic viscosity to mass density:

$$v = \mu / \rho \qquad (14\text{-}2)$$

Where μ is the *dynamic* viscosity and ρ the density. The unit is usually given in centistoke (10^{-6} m^2/s).

14.1 Wax precipitation

With falling temperature, heavy hydrocarbon components may precipitate as wax crystals. In pure form, some of these components will appear as solids at room temperature. Figure 14-2 shows experimental data for different hydrocarbon types as a function of molecular weight. In addition to the increase in melting point with molecular weight, it is notable that n-alkanes have the largest melting point in the whole range of molecular weights. However, when these components are present in mixtures, the melting points will be supressed to an extent depending on the concentration of the given components and other components in the mixture (the heavier components are dissolved in the lighter fractions). The prediction of wax precipitation with falling temperatures thus requires knowledge of the total composition of the mixture, in addition to certain physical-chemical properties of these components (Lira-Galeana, Firoozabadi, & Prausnitz, 1996).
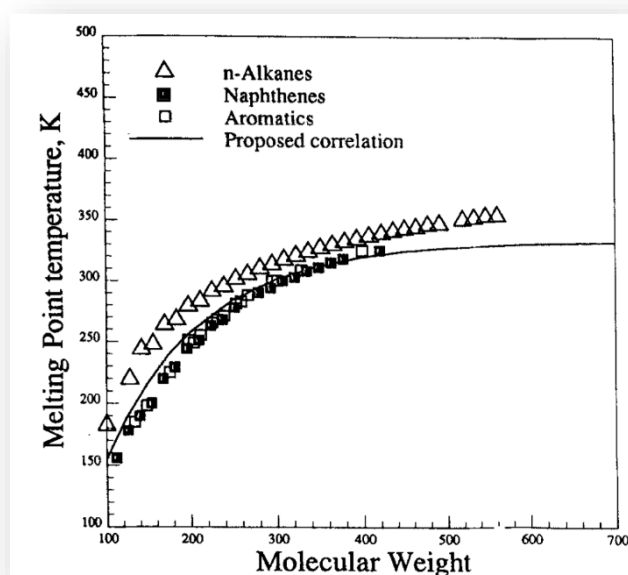
PROJECT NO.
302002226

REPORT NO.
OC2017 A-181

VERSION
2.0

34 of 49

Figure 14-2 Melting point temperatures of hydrocarbons (from Lira-Galeana et al. 1996).

The wax appearance temperature (WAT) is the temperature at which the first wax crystals start to form, on cooling of paraffin/solvent systems. As the temperature is lowered below the wax appearance temperature (WAT), more wax is gradually precipitated in solid form (wax crystals).

There are a number of different WAT determination methods, including: density and viscosity variation, differential scanning calorimetry, laser dispersion, and chromatography.

In the differential scanning calorimetry (DSC) method, the measurement of the heat released during solidification of paraffin crystals is the base to determine the wax appearance temperature. However, this technique can indicate WAT values which are lower than the real ones, mainly for crude oils with low paraffin content (Neto, Gomes, Neto, Dantas, & Moura, 2009).

In viscosimetry, the viscosity is determined at different temperatures. The WAT of the crude oil is estimated by plotting viscosity values versus reciprocal temperature. At temperatures above WAT the viscosity is found to be independent of shear rate (Newtonian behaviour), while at lower temperatures, the viscosity will increase significantly with reduced shear rate $\dot{\gamma}$. Typically, the wax appearance temperature is determined as the temperature where the data begin to deviate from linearity. As in DSC, viscosimetry can provide values for the WAT that are lower than the real ones.

Waxy crudes will show non-Newtonian behaviour at temperatures below the wax appearance temperature. This implies that the measured viscosity will be dependent on the shear rate in addition to the temperature. Figure 14-3 shows typical viscosity-temperature charts for waxy crudes. The dashed line of the graph in the figure represents the expected temperature variation in viscosity with Newtonian behaviour at temperatures below WAT (assuming that there is no precipitated wax). The line can be predicted from curve fitting of measured viscosity vs. temperature data above and below the wax appearance temperature ("temperature sweep").
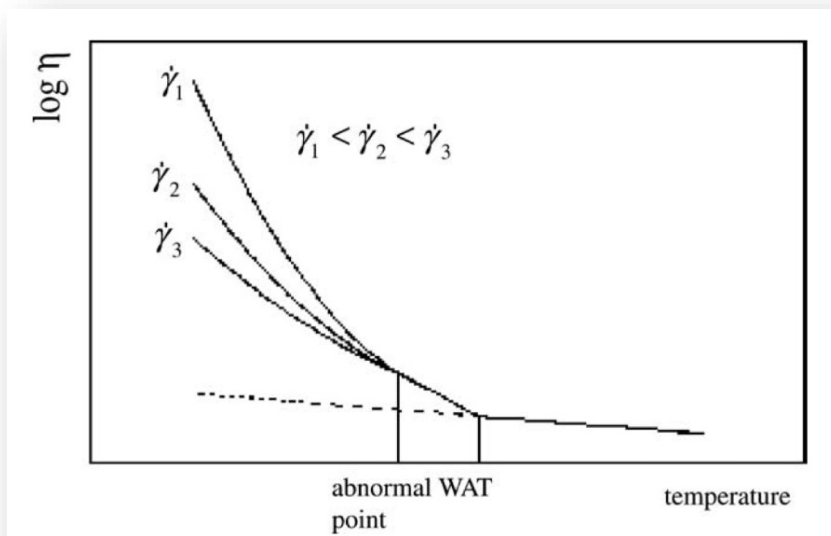
Figure 14-3 Typical viscosity vs. temperature chart for waxy crudes (after Li & Zhang, 2003).

Water-free oil at temperatures above the wax appearance temperance will behave Newtonian.

Thermodynamic models can be used to determine the equilibrium phase composition (vapour, liquid, solid) at a given temperature (Figure 14-4). The figure shows that the precipitation of wax is initiated as the oil is cooled to temperatures below about 300 – 310 K, which corresponds to 30 – 40⁰ C.
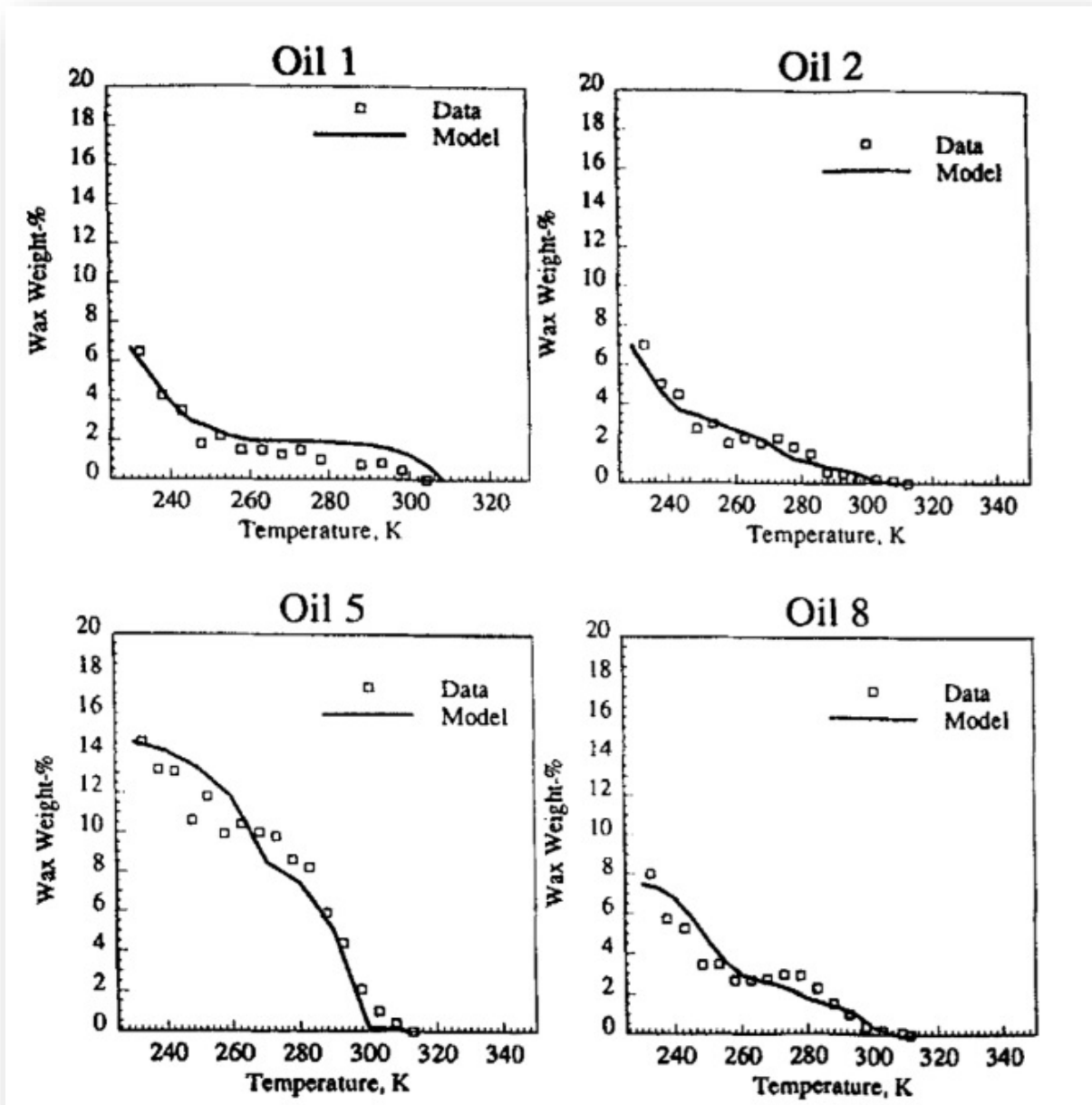
Figure 14-4 Experimental and predicted wax-precipitation for four oils (from Lira-Galeana et al., 1996).

Wax appearance temperature (WAT) is used synonymously with wax precipitation temperature (WPT) or cloud point. It is affected by salinity, being generally lower in more saline fluids.

PROJECT NO.
302002226

REPORT NO.
OC2017 A-181

VERSION
2.0

37 of 49

14.2 Shear-dependent computation of viscosity

In the cases of non-Newtonian behaviour of oil at temperatures below WAT, different models can be applied to compute viscosity: Ostwald de Waele (Power), the Bingham model or Ideal plastic, and the Herschell-Bulkley model.

Ostwald de Waele–relationship of shear stress, shear rate and viscosity

A Power-law fluid, or the Ostwald–de Waele relationship, is a type of generalized Newtonian fluid for which the shear stress, τ, is given by

$$\tau = K \left(\frac{\partial u}{\partial y} \right)^n \tag{14-3}$$

where:

- K is the *flow consistency index* (SI units Pa s^n),
- $\partial u / \partial y$ is the shear rate $\dot{\gamma}$ or the velocity gradient perpendicular to the plane of shear (SI unit s^{-1}), and
- n is the *flow behaviour index* (dimensionless).

The quantity

$$\mu_{eff} = K \left(\frac{\partial u}{\partial y} \right)^{n-1} \tag{14-4}$$

represents an apparent or effective viscosity as a function of the shear rate (SI unit Pa•s).

Also known as the Ostwald–de Waele power law, this mathematical relationship is useful because of its simplicity but only approximately describes the behaviour of a real non-Newtonian fluid.

Bingham or Ideal plastic model for yield stress and viscosity

A Bingham plastic is a viscoplastic material that behaves as a rigid body at low stresses but flows as a viscous fluid at high stress. It is named after Eugene C. Bingham who proposed its mathematical form. Mayonnaise is a Bingham plastic as well as toothpaste and slurries. Non-Newtonian oils might be described as a Bingham fluid.
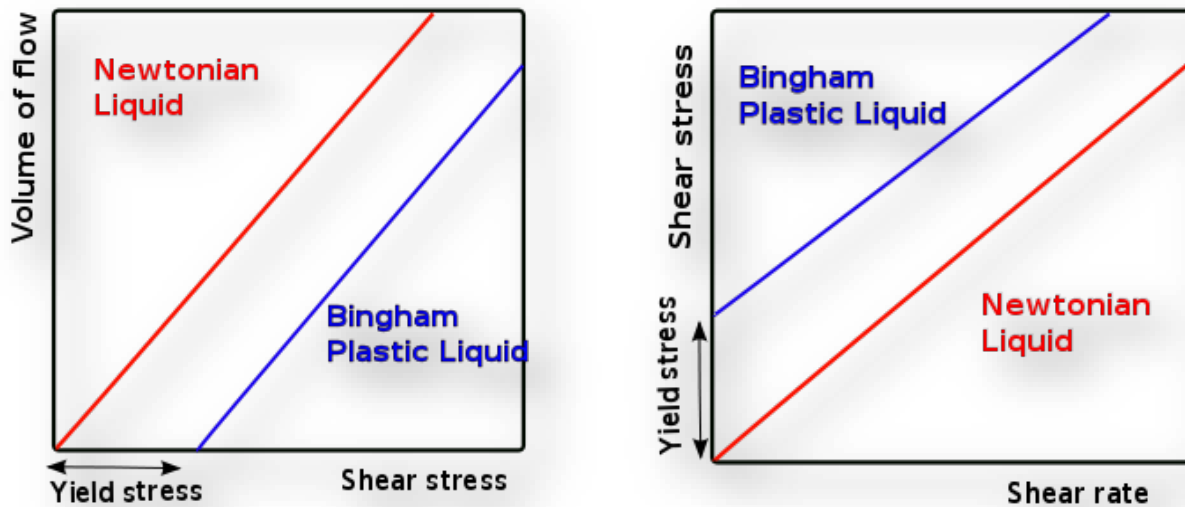
PROJECT NO.
302002226

REPORT NO.
OC2017 A-181

VERSION
2.0

38 of 49

Figure 14-5 Relationship of shear stress and volume of flow (left figure) and shear rate and shear stress for Bingham plastic liquids.

The graph on the right shows shear stress on the vertical axis and shear rate on the horizontal one. (Volumetric flow rate depends on the size of the pipe, shear rate is a measure of how the velocity changes with distance. It is proportional to flow rate, but does not depend on pipe size.) As before, the Newtonian fluid flows and gives a shear rate for any finite value of shear stress. However, the Bingham Plastic again does not exhibit any shear rate (no flow and thus no velocity) until a certain stress is achieved. For the *Newtonian fluid* the slope of this line is the *viscosity*, which is the only parameter needed to describe its flow. By contrast the *Bingham Plastic* requires two parameters, the *yield stress* <u>and</u> *the slope of the line,* known as the plastic viscosity.

Herschel - Bulkley model

The Herschel – Bulkley fluid is a generalized model of a non-Newtonian fluid, in which the strain experienced by the fluid is related to the stress in a *non-linear* way. Three parameters characterize this relationship: the consistency k, the flow index n, and the yield shear stress τ_0.

The constitutive equation of the Herschel- Bulkley model is commonly written as

$$\boldsymbol{\tau = \tau_0 + k\dot{\gamma}^n} \qquad (14\text{-}5)$$

where τ is the shear stress, $\dot{\gamma}$ the shear rate, τ_0 the yield stress, k the consistency index, and n the flow index. If $\tau < \tau_0$ the Herschel- Bulkley fluid behaves as a solid, otherwise it behaves as a fluid. For *n<1* the fluid is shear-thinning, whereas for *n>1* the fluid is shear-thickening. For *n=1* and $\tau_0 = 0$, this model reduces to the Newtonian fluid.
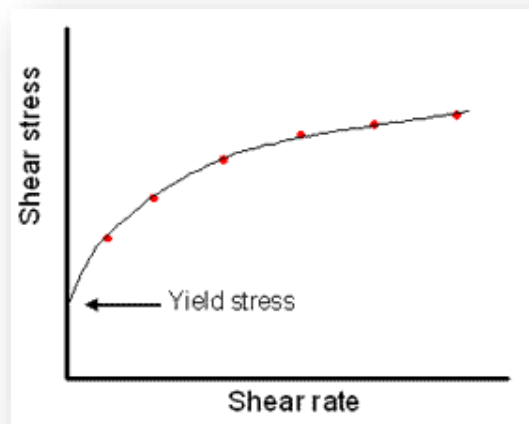
Figure 14-6 Shear thinning behaviour of a non-Newtonian fluid, viscosity decreasing with increasing shear rate. Shear thickening would mean the opposite behaviour with increasing viscosity.

All the models described above are valid for a constant given temperature.

14.3 Temperature-dependent computation of viscosity

The *ASTM-formula* and *the Arrhenius equation* are two commonly used formulas for temperature adjustment of viscosity of crude oil:

The ASTM-formula is expressed as follows:

$$ln[ln(v + c)] = A - B\ ln(T), \qquad (14\text{-}6)$$

while the Arrhenius type equation can be written as:

$$ln(v) = a + b\ {1000}/{T} \qquad (14\text{-}7)$$

where ln is the natural logarithm with base e, v is the kinematic viscosity in cSt, $c = 0.7$ and T is the absolute or thermodynamic temperature in Kelvin. *A, B, a, and b* are empirical coefficients.

Li and Zhang developed a simple correlation model for prediction of the viscosity as a function of shear rate and temperature as an ASTM-type formula, which in principle can be written as

$$\boldsymbol{\mu = \mu_0[1 - K(\dot{\gamma})c]^{-2.5}} \qquad (14\text{-}8)$$

where μ_0 is the expected Newtonian viscosity at the given temperature, c is the mass fraction of precipitated wax in the oil, and $K(\dot{\gamma})$ is an empirical function fitted to measured viscosity data. The ratio μ/μ_0 is defined as the relative viscosity μ_r. K can be related to the shear rate by a function of the type $K = C\ \dot{\gamma}^{-\alpha}$, where C and α are empirical coefficients. The study showed excellent fits with data for individual oils, however, the coefficients in the *K*-function were found to vary significantly (and unpredictably) between different oils.

Farah, Oliveira, Caldas, & Rajagopal (2005) presented an empirical model for prediction of the viscosity of water-in-oil emulsions, which may also be applied to water-free oils. The authors obtained viscosity data above and below the cloud-point, and derived different coefficients for the two cases of the ASTM formula for the

PROJECT NO.
302002226

REPORT NO.
OC2017 A-181

VERSION
2.0

40 of 49

temperature variation (i.e. A and B vs. A' and B', respectively). The values of these coefficients were found to vary proportionally with the volumetric water content W of the emulsion, such that

$$A = k_1 + k_2\,W \text{ and } B = k_3 + k_4\,W. \tag{14-9}$$

Farah et al. focused on variations with water content, and did not deal explicitly with variations in the coefficients with shear rate. With available data from temperature sweeps with water free oils at different shear rates, the shear rate dependency of the coefficients should be possible to determine, i.e. $A = f(\dot{\gamma})$ and $B = g(\dot{\gamma})$, where f and g are functional relations to be determined. This could provide a method for representing rheological data sets of waxy oils that does not require measured values for precipitated wax concentrations.

The current version of OSCAR implements an Arrhenius equation with reference to the NRDAM database. A simplified version of the ASTM-formula is used in OWM, with $c = 0$ and a linear relationship with T (T instead of $\log(T)$) at the right hand side of the equation. A comparison of these two equations can be found in Appendix B.

15. Solidification of waxy crude oils and condensates

Oil on the sea surface does not have to have its origin from a surface spill but may result from a sub-surface release. Surfacing oil will cause a slick that can be downstream to the source, depending on droplet sizes, gas-to-liquid-ratio (GOR, GLR) and environmental conditions.

Plumes from oil and gas blowouts from moderate depths (less than 300 - 400 m) will in general surface and produce thin oil slicks at the sea surface. While the spreading of surface oil from higher depth with trapped plumes depend on the droplet sizes of the surfacing oil and ambient currents, oil slick thickness and spreading from surfacing plumes will be governed by the radial outflow of the entrained water. The extent will depend on the oil flow rate, the Gas to Oil Ratio (GOR) and the water depth as demonstrated in Fanneløp's early studies of the hydrodynamics of underwater blowouts (Fanneløp & Sjøen, 1980).

With discharges of waxy crude oils or condensates with high pour points, the oil droplets formed at the outlet may solidify during the rise to the surface in the cold seawater. When such solidified droplets arrive at the surface, they will form a sparse field of floating oil particles rather than a continuous oil film. However, the solidified droplets might merge and "condense" into a continuous slick if the surface coverage exceeds the surface coverage of a monolayer of oil droplets.

Computation of surface coverage of "solidified" oil droplets

For monodispersed oil droplets with diameter d, the fraction of the surface area covered with oil, Φ, corresponding to a given surface oil concentration C (m³/m²) will be $\Phi = 3/2\ C/d$. This is found by defining Φ as the projected area of the number of droplets N contained in the oil volume covering an area A of the sea surface, i.e. $\Phi = N \times a/A$, where $a = \pi/4\ d^2$, $N = C\ A/v$, and $v = \pi/6\ d^3$.

For droplets with a given size distribution, the surface coverage can then be expressed by the equation

$$\Phi = 3/2\ C/d_H, \tag{15-1}$$

where d_H is the harmonic mean droplet size of corresponding to the given size distribution. For lognormal distributions, the harmonic mean droplet size is given by the equation (Limbrunner, Vogel, & Brown, 2000):

$$d_H = e^{(\mu - 1/2\sigma^2)} \tag{15-2}$$

where $\mu = \ln(d_{50})$, where d_{50} is the volume median droplet diameter. Recent studies of droplet breakup in oil jets show mean values σ of 0.78 in natural logarithmic units (Johansen et al. 2013), corresponding to harmonic mean diameters of about 0.7 times the volume median diameter.

PROJECT NO.
302002226

REPORT NO.
OC2017 A-181

VERSION
2.0

41 of 49

Figure 15-1 shows the variation in the covered surface area Φ with volume median droplet diameter for a range of surface oil concentrations. The values are computed with Equation (15—1), presuming a lognormal droplet size distribution with $\sigma = 0.78$. For monodispersed droplets, the surface concentration may reach about 87 % in a monolayer (hexagonal packing), but with assorted droplet diameters, the upper limit for a monolayer may be higher, but still limited by 100 %.
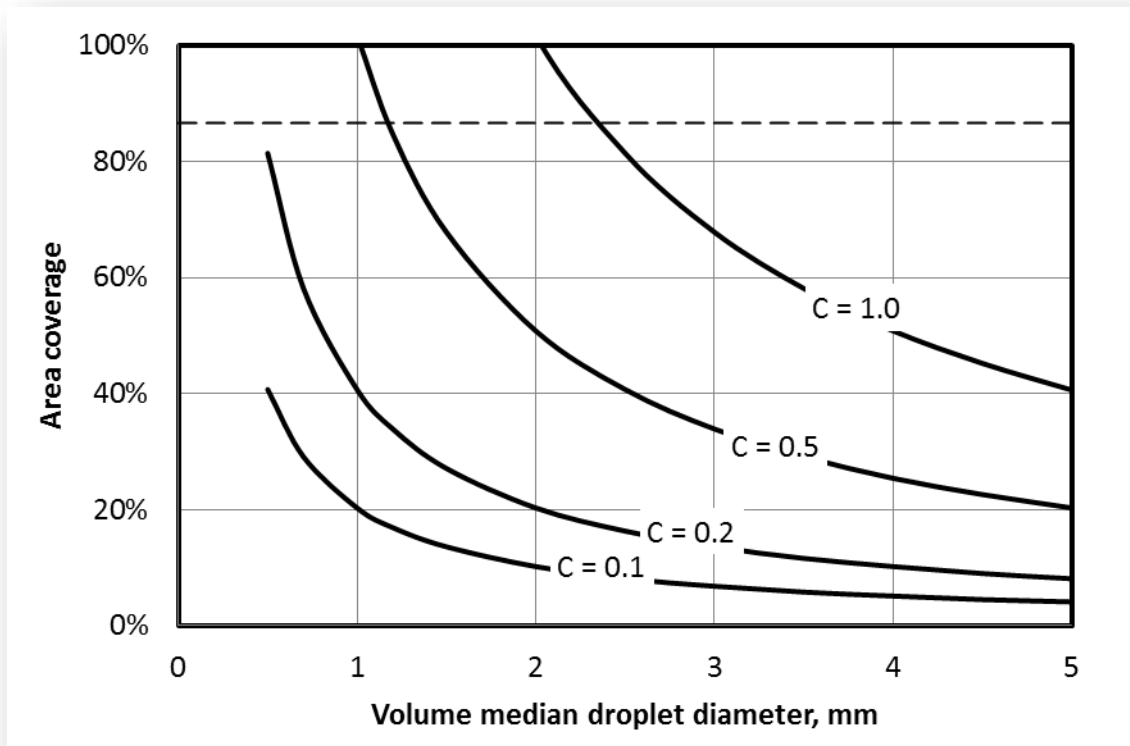

Figure 15-1 Surface area coverage computed for lognormal distributions with volume median droplet diameters from 0.5 to 5 mm and surface oil concentrations C in the range from 0.1 to 1 m³/m². The dashed line corresponds to a single layer of densely packed monodispersed droplets.

Separation distance for computed surface coverage

The results demonstrate that with typical surface oil concentrations and droplet sizes for subsea blowouts from moderate water depths, ($C < 0.1$ m³/m², $d_{50} > 1$ mm), the oil surface coverage will be well below the limit for a close-packed monolayer. However, even with surface coverages in the range below 10%, the floating solidified droplets may be close enough to be submitted to coalescence due to turbulent motions on the sea surface. The mean droplet separation distance R_m can be estimated from the number of droplets N per unit area, as expressed by the equation

$$R_m^2 = {}^1\!/_N \qquad\qquad (15\text{—}3)$$

where

$$N = C\,{}^6\!/_\pi \sum {}^{\Delta V_i}\!/_{d_i^3} \equiv C\,{}^6\!/_\pi\, d_N^{-3} \qquad\qquad (15\text{—}4)$$

PROJECT NO.
302002226

REPORT NO.
OC2017 A-181

VERSION
2.0

42 of 49

and d_N is an equivalent number diameter. For a lognormal distribution, this diameter is given by the equation:

$$d_N = e^{(\mu - 3/2\sigma^2)} \qquad (15—5)$$

Figure 15-2 shows mean separation distances computed for surface oil concentrations in the range representative for subsea oil and gas blowouts from moderate water depths ($C < 0.1$ mm). The computed distances are found to be in the same order of magnitude as the volume median diameter d_{50}, i.e. from about one to a maximum of 6 times d_{50} in the chosen range of surface oil concentrations. In such cases, it is probable that the turbulent motions in the water surface may cause smaller droplets to be swept up by larger ones, eventually forming patches of oil droplet aggregates.
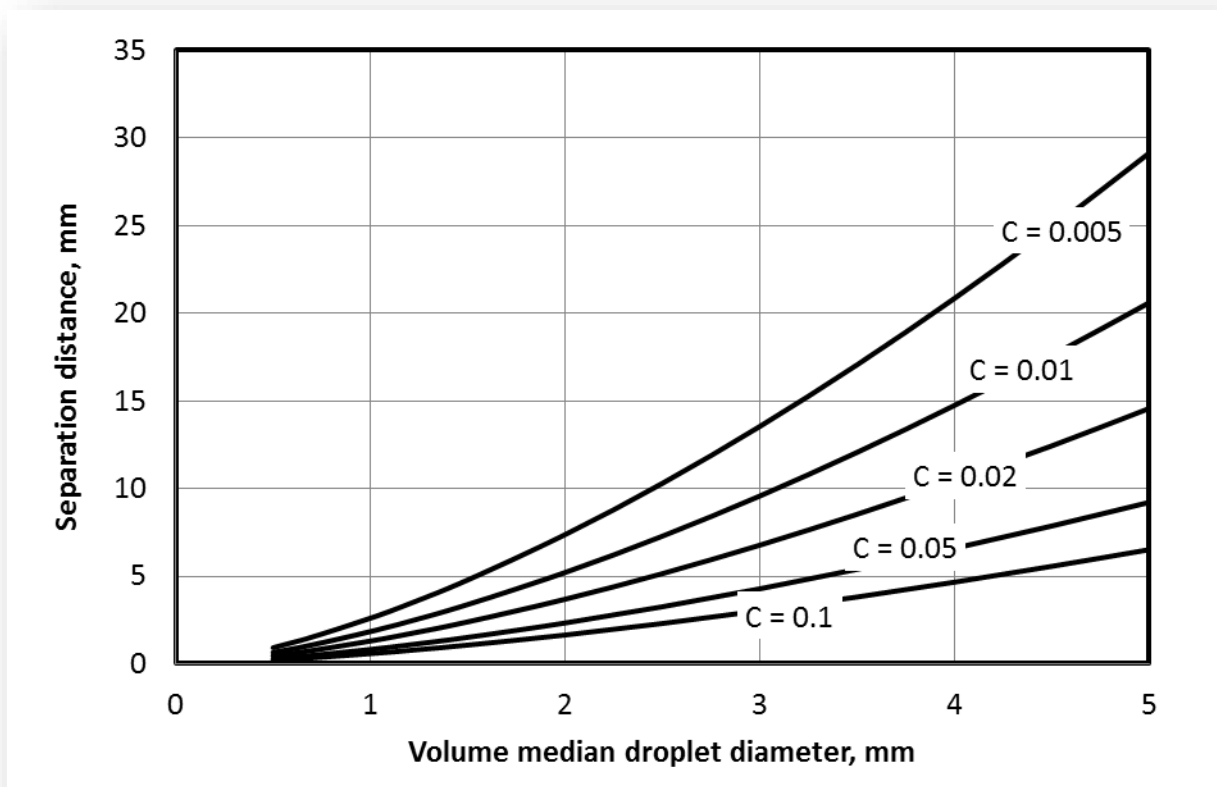

Figure 15-2 Mean separation distance between floating droplets as a function of volume median droplet diameter for a range of surface oil concentrations, $C = 0.01$ to 0.1 mm. The oil droplets are presumed to follow a lognormal distribution with σ = 0.78.

It is unknown if wave action (breaking waves) will cause the droplet aggregates to break up into the "original" droplet sizes again, or if different droplet size distributions would be formed. This will depend on whether the aggregates have merged into a homogeneous slick, or rather consist of loosely connected solidified "droplets".

Laboratory experiments where floating droplet aggregates are submitted to breaking waves or falling water jets, similar to the experiments conducted to determine droplet size distributions formed by breaking waves on floating oil slicks (Johansen et al. 2015) will be able to help answering these questions but are out of scope of this project.

16. Conclusion

At temperatures below wax appearance temperature and near the pour point of oil, wax precipitation effects will be more pronounced, especially for waxy oils.

Spreading and subsequent transport

A proposed methodology from Farah et al. (see 14.3) provides a possibility to calculate temperature dependent viscosity. The method will have to be calibrated with data from temperature sweep experiments for different types of oil, preferably including emulsions, weathered oil and model oils. Useful data-sets may already be available for different oils, but a systematic rheological study of a selection of waxy crude oils will be useful for testing the applicability of the model presented here.

Including oil viscosity and yield stress will allow determining equilibrium / terminal film thickness for an oil slick and the transition from a spreading to a transport regime (break-up into patches).

Spreading modelling should account for the differences in the spreading behavior of instantaneous and continuous releases, respectively, and compute different slick thickness with distance from the release, if possible.

Solidification of oil on the way to and on the sea surface

(Waxy) oils may solidify at temperatures close to pour point and build (semi-) solidified lumps rather than a continuous film. Calculations of possible values for coverage and separation distances between these lump show that despite low coverage rates solidified lumps are likely to constantly combine and break-up due to the turbulent motion of the surface water. The time scale for this as well as the further fate and "droplet" size distributions are unknown and require further experimental work before this process can be included into modelling of surface oil.

17. Recommendation

In agreement with the recommendations from Part II we recommend the following further development / improvement of the OSCAR oil spill model:

1) Resolution: surface oil needs to be represented by a sufficient number of spillets (numerical particles) and grid cells (numerical units) to capture the thickness in different areas of a surface slick.
2) Rheological properties: effects of oil viscosity and yield stress (see chapter 14) and termination of spreading need to be included into the spreading model.
3) Linking with shear spreading: Spreading on the sea surface needs better alignment with sub-surface spreading and resurfacing of oil.
4) Slick thickness distribution: differences in thicknesses need to be reported to the model user (to compare to thicknesses as observed from spill experiments and accidents).
5) Termination: needs to be determined automatically and to cause the spreading regime to switch to the generation of patches instead of continuous homogeneous films.

Subsurface releases and their initial radial spreading on the sea surface are accounted for in OSCAR via Plume3D.

Modelling spreading of oil in dependency of temperature / viscosity (yield stress)

The improved temperature handling within the OSCAR model will enable determination of the transition from Newtonian to non-Newtonian behaviour by relating water temperature to oil temperature and computing temperature dependent viscosities.

Experiments have determined viscosities for different shear rates and the property yield stress can be computed from these using a Bingham approach. The results from these experiments may be used to validate / calibrate the proposed methodology for computation of temperature and shear dependent oil viscosity further in the future.

Shear dependent oil viscosities will be included into the set of possible input data for the OSCAR model and will allow including of yield stress into equations for viscous- gravity spreading. Possible non-Newtonian behaviour of weathered oil (determined by this yield stress) will terminate surface spreading (when gravitational forces cannot overcome yield stress and viscous forces) and determine a terminal film thickness.

Surface oil can now be reported by thickness classes, e.g. Bonn agreement thicknesses, to determine recoverable oil from the new output file (netCDF surface grid).

Modelling of solidified oil

It was discussed that the oil residue changes from being a single liquid phase above pour point to being two phases (solid wax and liquid oil) below its pour point. The proposal was to model these phases separately; one model for the wax and one for the liquid fraction of the oil.

It is known that the solid wax will be physically much more persistent that the liquid oil, and both phases will eventually be biodegraded, but the wax might persist long enough as small particles to reach the shore. Since there are so many unknowns with respect to fate and behaviour of solidified oil we do not see the possibility of including it into oil spill modelling at this stage.

Linking with shear spreading: alignment of surface spreading with sub-surface spreading and resurfacing of oil

Future development should improve the link between resurfacing oil and surface signature. Current model implementations do not address physical (rheological) properties of resurfacing oil, which might have unfortunate effects in regimes with high mixing in terms of overly pronounced spreading.

The surface signature of an oil spill is interlinked with many other processes and the modelling of surface oil is therefore highly interlinked with the modelling of other processes (sub models). Affected sub models include all processes, which change the mass of the oil on the sea surface, as e.g. natural dispersion, evaporation, emulsification and biodegradation. As these processes are sensitive to other oil properties, changes must be considered and calibrated carefully.

PROJECT NO.
302002226

REPORT NO.
OC2017 A-181

VERSION
2.0

45 of 49

References

References Part I

Assaf, G. R. Gerard and A. L. Gordon. 1971. Some mechanisms of oceanic mixing revealed in photographs. *J. Geophys. Res*. **76**, 6550 - 6572.

Audunson, T., H. K. Celius, Ø. Johansen, P. Steinbakke and S. E. Sørstrøm. 1984. The experimental oil spill on Haltenbanken 1982. IKU/SINTEF report Publication No. 112, December 1984. ISSN 0332-5288.

Craik, A.D.D. 1977. The generation of Langmuir circulations by an instability mechanism. *Journal of Fluid Mechanics*, **81**(2):209-223.

Csanady, G. T. 1973. *Turbulent Diffusion in the Environment*. Reidel. 248 pp.

Daling Per S., Merete Øverli Moldestad, Øistein Johansen, Alun Lewis & Jon Rødal. 2003. Norwegian Testing of Emulsion Properties at Sea—The Importance of Oil Type and Release Conditions. Spill Science & Technology Bulletin, Vol. 8, No. 2, pp. 123–136, 2003

Faller, A. J. and A. H. Woodcock. 1964. The spacing of windrows of sargassum in the ocean. *J. Mar. Res*., 22, 22 - 29

Faller, A. J. and E. A. Caponi. 1978. Laboratory studies of wind-driven langmuir circulations. *J. Geophys. Res.*, **83**, 3617 - 3633

Faller, A. J. and S. J. Auer. 1988. The roles of Langmuir circulation in the dispersion of surface tracers. *J. Phys. Oceanogr.,* **18**, 1108 - 1123.

Graham, A. and A.J. Hall. 1997. The horizontal distribution of bubbles in a shallow sea. *Continental Shelf Research,* **17**(9):1051-1082.

Kenney, B. C. 1979. An experimental investigation of the fluctuating currents responsible for the generation of wind rows. Ph. D. thesis. University of Waterloo, 163 pp.

Langmuir, I., 1938. Surface water motion induced by wind. *Science*, **87**, 119 - 123.

Lehr, W. J. and Debra Simecek-Beatty, 2000. The Relation of Langmuir Circulation Processes to the standard Oil Spill Spreading, Dispersion and Transport Algorithms. *Spill Science & Technology Bulletin*, Vol. 6 No. 3/4, pp 247-253, 2000

Lehr, W. J. 2010. Spreading. https://crrc.unh.edu/.../SPREADING%20(Bill%20Lehr)01.20.10.doc

Leibovich, S. 1977. Convective instability of stably stratified water in the ocean. *Journal of Fluid Mechanics, 82:561-581.*

Leibovich, S. 1977. Convective instability of stably stratified water in the ocean. *Journal of Fluid Mechanics*, 82:561-581.

Leibovich, S. 1983. The form and dynamics of Langmuir circulation. *An. Rev. Fluid. Mech.*, **15**, 391 - 427

Melbye, A.G, Johansen, Ø., Resby, J.L.M, M.Ø Moldestad: 1999: Thin oil films of Norne Crude; Phase 1&2 Small-scale laboratory and meso-scale flume tests on fate of thin oil films. SINTEF report STF66 F99062. Confidential

Nimmo Smith, William Alexander Michael. 2000. Dispersion of Material by Wind and Tide in Shallow Seas. Doctor of Philosophy. School of Ocean and Earth Science Faculty of Science. September 2000

PROJECT NO.
302002226

REPORT NO.
OC2017 A-181

VERSION
2.0

46 of 49

Pollard, R. T. 1977. Observations and theories of Langmuir circulation and their role in near surface mixing. *A Voyage of Discovery; G. Deacon 70th anniversary Volume*, M. Angel, Editor. Pergamon, 235 - 251.

Rye, H., P. J. Brandvik, T. Strøm. 1997. Subsurface Blowouts. Results from Field Experiments, Spill Science and Technology Bulletin 4 (4), 239 - 256.

Rye, H. 2000. Probable Effects of Langmuir Circulation Observed on Oil Slicks in the Field. Spill Science & Technology Bulletin. Vol. 3/4, pp 263-271.

Smith, J., R. Pinkel and R. A. Weller. 1987. Velocity structure in the mixed layer during MILDEX. *J. Phys. Oceanogr.*, 17, 425 - 439

Smith, J.A. 1982. Observed growth of Langmuir circulation. *Journal of Geophysical Research*, **97**(C4):5651-5664.

Sørstrøm, S. E. 1989. 1989 full scale experimental oil spill at Haltenbanken. Project description, methods and data presentation OCEANOR, Oceanic Company of Norway, Trondheim 15 August 1989.

Strommel, H. 1952. Streaks on natural water surfaces. *Weather*, 6, 72 -74

Thorpe, S. A. 1992. The break-up of Langmuir circulation and the instability of vortices. J. Phys. Oceanogr., 22, 350 - 360

Thorpe, S.A., M.S. Cure, A. Graham, and A. J. Hall. 1994. Sonar observations of Langmuir circulation and estimation of dispersion of floating particles. Journal of Atmospheric and Oceanic Technology, 11:1273-1294.

Weller, R. A. and J. F. Price. 1988. Langmuir circulation within the oceanic mixed layer. *Deep-Sea Res.,* 35, 711 - 747

Williams, K. C. 1965. Turbulent water flow patterns resulting from wind stress on the ocean. Mem. Rep. 1653, U.S. Naval Res. Lab Washington DC

References Part II & III

Csanady, G. T. (1973). *Turbulent Diffusion in the Environment*.

Fanneløp, T. ., & Waldman, G. D. (1972). Dynamics of Oil Slicks. *AIAA Journal*, *10*(4), 506–510. http://doi.org/doi: 10.2514/3.50127

Fanneløp, T. K., & Sjøen, K. (1980). Hydrodynamics of Underwater Blowouts. *Norwegian Maritime Research*, *4*, 17–33.

Farah, M. A., Oliveira, R. C., Caldas, J. N., & Rajagopal, K. (2005). Viscosity of water-in-oil emulsions: Variation with temperature and water volume fraction. *Journal of Petroleum Science and Engineering*, *48*(3-4), 169–184. http://doi.org/10.1016/j.petrol.2005.06.014

Farmer, D., & Li, M. (1995). Patterns of Bubble Clouds organized by Langmuir Circulation. *Journal of Physical Oceanography*. http://doi.org/10.1175/1520-0485(1995)025<1426:POBCOB>2.0.CO;2

Gjosteen, J. K. Ø. (2001). Oil Spreading In Cold Waters - A Model Suitable For Broken Ice. In *The Eleventh International Offshore and Polar Engineering Conference*.

Johansen, Ø. (2000). DeepBlow – a Lagrangian Plume Model for Deep Water Blowouts. *Spill Science & Technology Bulletin*, *6*(2), 103–111. http://doi.org/10.1016/S1353-2561(00)00042-6

Johansen, Ø., Reed, M., & Bodsberg, N. R. (2015). Natural dispersion revisited. *Marine Pollution Bulletin*, *93*(1-2), 20–6. http://doi.org/10.1016/j.marpolbul.2015.02.026

Johansen, Ø., Rye, H., & Cooper, C. (2003). DeepSpill—Field Study of a Simulated Oil and Gas Blowout in Deep Water. *Spill Science & Technology Bulletin*, *8*(5-6), 433–443. http://doi.org/10.1016/S1353-2561(02)00123-8

Lehr, W. J. (2001). Review of modeling procedures for oil spill weathering behavior. *Advances in Ecological Sciences*, *9*, 51–90.

Leibovich, S. (1983). The form and Dynamics of Langmuir Circulations. *Annual Review of Fluid Mechanics*, *15*(1), 391–427. http://doi.org/10.1146/annurev.fl.15.010183.002135

Leibovich, S. (1997). *Surface and Near-Surface Motion of Oil in the Sea*.

Li, H., & Zhang, J. (2003). A generalized model for predicting non-Newtonian viscosity of waxy crudes as a function of temperature and precipitated wax. *Fuel*, *82*(11), 1387–1397. http://doi.org/10.1016/S0016-2361(03)00035-8

Limbrunner, J., Vogel, R., & Brown, L. (2000). Estimation of Harmonic Mean of a Lognormal Variable. *J. Hydrol. Eng.*, *5*(1), 59–66.

Lira-Galeana, C., Firoozabadi, A., & Prausnitz, L. M. (1996). Thermodynamics of wax precipitation in petroleum mixtures. *AIChE Journal*, *42*, 239–248.

Liu, T., & Sheng, Y. P. (2014). Three dimensional simulation of transport and fate of oil spill under wave induced circulation. *Marine Pollution Bulletin*, *80*(1-2), 148–159. http://doi.org/10.1016/j.marpolbul.2014.01.026

McWilliams, J. C., & Sullivan, P. P. (2000). Vertical Mixing by Langmuir Circulations. *Spill Science & Technology Bulletin*, *6*(3-4), 225–237. http://doi.org/10.1016/S1353-2561(01)00041-X

Neto, D. a. a., Gomes, E. a. S., Neto, B., Dantas, T. N. C., & Moura, C. P. a. M. (2009). Determination of Wax Appearance Temperature (Wat) in Paraffin / Solvent Systems By Photoelectric Signal and. *Brazilian Journal of Petroleum and Gas*, *3*, 149–157.

Nimmo-Smith, W. A. M. (2000). *Dispersion of mterial by wind and tide in shallow seas*. University of Southhampton.

PROJECT NO.
302002226

REPORT NO.
OC2017 A-181

VERSION
2.0

48 of 49

Reed, M., Brandvik, P. E. R. J., Daling, P. E. R., Lewisà, A., Fioccoà, R., Mackay, D. O. N., & Prentki, R. (1999). Oil Spill Modeling towards the Close of the 20th Century : Overview of the State of the Art. *Spill Science & Technology Bulletin*, *5*(1), 3–16.

Reed, M., Gundlach, E., & Kana, T. (1989). A coastal zone oil spill model: development and sensitivity studies. *Oil and Chemical Pollution*, *5*(6), 411–449. Retrieved from http://www.sciencedirect.com/science/article/pii/S026985798980019X

Reed, M., Johansen, Ø., Brandvik, P. J., Daling, P., Lewis, A., Fiocco, R., … Prentki, R. (1999). Oil Spill Modeling towards the Close of the 20th Century: Overview of the State of the Art. *Spill Science & Technology Bulletin*, *5*(1), 3–16. http://doi.org/10.1016/S1353-2561(98)00029-2

Simecek-Beatty, D., & Lehr, W. J. (2000). Langmuir circulation and oil spill trajectory models workshop - Comments and recommendations. *Spill Science and Technology Bulletin*, *6*(3-4), 273–274. http://doi.org/10.1016/S1353-2561(01)00046-9

Skyllingstad, E. D. (2000). Scales of Langmuir Circulation Generated using a Large-Eddy Simulation Model. *Spill Science & Technology Bulletin*, *6*(3-4), 239–246. http://doi.org/10.1016/S1353-2561(01)00042-1

Thorpe, S. a. (2000). Langmuir Circulation and the Dispersion of Oil Spills in Shallow Seas. *Spill Science and Technology Bulletin*, *6*(3-4), 213–223. http://doi.org/10.1016/S1353-2561(01)00040-8

Venkatesh, S., El-Tahan, H., Comfort, G., & Abdelnour, R. (1990). Modelling the behaviour of oil spills in ice-infested waters. *Atmosphere-Ocean*, *28*(3), 303–329. http://doi.org/10.1080/07055900.1990.9649380

Yang, D., Chamecki, M., & Meneveau, C. (2014). Inhibition of oil plume dilution in Langmuir ocean circulation. *Geophysical Research Letters*, *41*(5), 1632–1638. http://doi.org/10.1002/2014GL059284

SINTEF

Technology for a better society